

Phenomenology of SUGRA Extensions of the Starobinsky Model

MAN Ping Kwan, Ellgan^{a)†}

Department of Pure and Applied Physics, Waseda University^{a)}

1 Abstract

We analyze BI-extended model in a complete form and compare the predictions with that of Starobinsky model. Under the parameter constraints in Planck 2018, we find that the dynamics of the whole inflation process described by BI-extended and Starobinsky models are nearly the same, even though there are some differences in the regions out of inflation. We also find the scales of parameters in BI-extended model and inflaton values at the first horizon crossing required to implement inflation. The changes of (n_s, r) fingerprints of BI-extended model and that of evolutions of inflaton field due to the variations of relevant parameters are also investigated.

2 Introduction

Slow-roll parameters	Range(s)	Spectral indices	Range(s)
ϵ_V	< 0.004	$n_s - 1$	$[-0.0423, -0.0327]$
η_V	$[-0.021, -0.008]$	$\alpha_s := \frac{dn_s}{d\ln k}$	$[-0.008, 0.012]$
ξ_V	$[-0.0045, 0.0096]$	$\beta_s := \frac{d^2 n_s}{d\ln k^2}$	$[-0.003, 0.023]$
H_{hc}	$< 2.7 \times 10^{-5} M_{\text{pl}}$	V_{hc}	$< (1.7 \times 10^{16} \text{ GeV})^4$

Table 1: Slow roll potential parameters and spectral indices in Planck 2018

Cosmological inflation is a powerful solution to the flatness and horizon problems at the beginning of the standard Big Bang scenario [3, 4, 5]. The constraints of observation data of Planck 2018 are listed in Table 1¹. All inflation models naturally provide the primordial density fluctuation and curvature perturbation, which can be observed by cosmic microwave (CMB) background [6, 7]. So far many models listed in [7, 8] can satisfy the observation. In particular, Starobinsky model (also called R^2 inflation model), motivated

⁰MAN Ping Kwan, Ellgan, E-mail: ellgan101@akane.waseda.jp

¹Note that V_{hc} in Table 1 is the scalar power spectrum at the first horizon crossing given by

$$V_{\text{hc}} = \frac{3\pi^2}{2} r M_{\text{pl}}^4 A_s|_{\text{hc}}, \quad (1)$$

where $A_s|_{\text{hc}}$ is the scalar power spectrum evaluated at the first horizon crossing.

by modified gravity [9, 10], provides the most promising prediction. This triggers many discussions about properties of Starobinsky models during and after inflation like [11] and the counterparts of Starobinsky like models such as [12] and [13], and the dynamics of the extensions of Starobinsky model such as [14] and [15].

On the other hand, it is vital to integrate those inflation models to high energy theories like supergravity (SUGRA). So far, SUGRA, which is a locally supersymmetric theory, has been an appropriate model to unify gravity with particle physics beyond the Standard Model of elementary particles and beyond the Standard Model of cosmology [35]. In particular, the F -term potential in SUGRA provides many insights in α attractor property, which is describing the connection between Starobinsky model and various power-law model in the graph of tensor-to-scalar ratio against spectral index [16, 17, 18, 19, 20, 21].

Although there is an obstacle called η problem resulting from the factor $e^{\frac{K}{M_{\text{Pl}}^2}}$ in the F -term potential where K denotes Kähler potential [22], it was solved by making a proper choice in super-potential and Kähler potential as shown in [23] and [24]. Another solution is discussed in [25] and [26], which considers the scalar component of a massive $U(1)$ vector multiplet as an inflaton field. This can avoid the occurrence of η problem and realize inflation in a simple way.

It is natural to consider the UV completion of SUGRA inflation models. One possibility is to adopt Dirac-Born-Infeld (DBI) action, which carries zero-mode vector fields attached to the D -branes [27, 28]. The supersymmetric (SUSY) version of DBI action was studied in [29] and [30]. The matter coupled DBI type action including a matter charged under $U(1)$ symmetry is discussed in [33]. The action of the massive vector multiplet is extended to the DBI type action, which can be constructed by the DBI action of a massless vector multiplet coupled to a Stueckelberg multiplet with $U(1)$ symmetry [34], leading to the DBI extension of Starobinsky model and the corresponding dual action², with the inflaton field being stored in the lowest scalar component of a massive vector multiplet. This model was also studied in [35], and the effective scales are evaluated under the approximation of the square root term and compared with that of Starobinsky model, with the assumption that the inflaton field is induced from the scalar curvature by the Legendre transformation instead of the scalar field of the massive vector multiplet.

Thus, in this paper, we study the version of [35] in a complete form³ to see how all the higher order terms contribute to the predictions. For the rest of this paper, we call the model we are going to study as "BI-extended model", although there are many meanings for "BI" like "Brane Inflation"[38] and DBI inflation [39]. In section 3, we introduce the basic formalism of obtaining the potential from a general $F(R)$ term in a Lagrangian density. After a short review in Starobinsky model in section 4, we analyze

²The duality described here is originated from [30].

³We assume the inflaton field is from the scalar curvature instead of the scalar field of the massive vector multiplet.

the BI-extended model in section 5. In section 6, we show the possible parameters and inflaton values at the first horizon crossing ϕ_{hc} in Starobinsky model and BI-extended model based on the observation constraints listed in Table 1 and how BI-extended model changes as g and β vary. In section 7, we demonstrate the evolutions of inflaton field as cosmic time t runs in different choices of g and β . Finally, we discuss our results in section 8 and summarize them in section 9.

3 Basic Formalism for studying inflation with $F(R)$ model

In this section, we are going to review the basic derivation of $F(R)$ ⁴ theory⁵. Note that the Lagrangian is given by

$$S_{\text{Jordan}} = \frac{M_{\text{pl}}^2}{2} \int d^4x \sqrt{-\tilde{g}} F(\tilde{R}) \quad (2)$$

where $\tilde{g}_{\mu\nu}$ is the metric in the Jordan frame⁶. To get the equation of motion (E.O.M.), we vary the action with respect to the metric $\tilde{g}^{\mu\nu}$ to produce

$$F'(\tilde{R})\tilde{R}_{\mu\nu} - \frac{1}{2}F(\tilde{R})\tilde{g}_{\mu\nu} - [\nabla_\mu \nabla_\nu - \tilde{g}_{\mu\nu}\square] F'(\tilde{R}) = \frac{1}{M_{\text{pl}}^2} \tilde{T}_{\mu\nu}, \quad (3)$$

where $F''(\tilde{R}) \neq 0$ and $\tilde{T}_{\mu\nu}$ is the energy-momentum tensor in the Jordan frame. Also, by taking Legendre Transformation and introducing the new scalar field χ , we have

$$F(\tilde{R}) = F'(\chi)(\tilde{R} - \chi) + F(\chi). \quad (4)$$

In order to change it from Jordan frame to Einstein frame, we adopt the following conformal transformation

$$\tilde{g}_{\mu\nu} = \Omega^2(x) g_{\mu\nu} \quad (5)$$

where $\Omega(x)$ is a function of the space-time coordinates. Note that the Christoffel symbols, Riemann tensor, Ricci tensor and Ricci scalar in the Jordan frame can be written in terms

⁴Note that the mass scale of $F(R)$ is $[F(R)] = M_{\text{pl}}^2$, where M_{pl} is the reduced Planck mass.

⁵For general review, please refer to [31].

⁶In this paper, notations with a tilde mean the corresponding quantities evaluated in the Jordan frame.

of the counterparts in the Einstein frame as follows

$$\begin{aligned}
\tilde{\Gamma}_{\mu\nu}^\rho &= \Gamma_{\mu\nu}^\rho + (\delta_\mu^\rho \partial_\nu \ln \Omega + \delta_\nu^\rho \partial_\mu \ln \Omega - g_{\mu\nu} \partial^\rho \ln \Omega), \\
\tilde{R}^a_{bcd} &= R^a_{bcd} - 2 \left(\delta_{[c}^a \delta_{d]}^f \delta_b^f - g_{b[c} \delta_{d]}^e g^{af} \right) \frac{\nabla_e \nabla_f \Omega}{\Omega}, \\
&\quad + 2 \left(2\delta_{[c}^a \delta_{d]}^e \delta_b^f - 2g_{b[c} \delta_{d]}^e g^{af} + g_{b[c} \delta_{d]}^a g^{ef} \right) \frac{(\nabla_e \Omega)(\nabla_f \Omega)}{\Omega^2}, \\
\tilde{R}_{bc} &= R_{bc} - \left[(d-2)\delta_b^f + g_{bc} g^{ef} \right] \frac{\nabla_e \nabla_f \Omega}{\Omega} + \left[2(d-2)\delta_b^f \delta_c^e - (d-3)g_{bc} g^{ef} \right] \frac{(\nabla_e \Omega)(\nabla_f \Omega)}{\Omega^2}, \\
\tilde{R} &= \frac{R}{\Omega^2} - 2(d-1)g^{ef} \frac{\nabla_e \nabla_f \Omega}{\Omega^3} - (d-1)(d-4)g^{ef} \frac{(\nabla_e \Omega)(\nabla_f \Omega)}{\Omega^4}.
\end{aligned} \tag{6}$$

where d is the dimension of the space-time. Hence, in four dimension ($d = 4$), we can change all the variables from the Jordan frame to the Einstein frame

$$\begin{aligned}
S_{\text{Einstein}} &= \frac{M_{\text{pl}}^2}{2} \int d^4x \sqrt{-g} \left\{ R - \frac{3}{2} \left(\frac{F''(\chi)}{F'(\chi)} \right)^2 g^{\mu\nu} \partial_\mu \chi \partial_\nu \chi - \left[\frac{\chi}{F'(\chi)} - \frac{F(\chi)}{F'(\chi)^2} \right] \right\} \\
&= \int d^4x \sqrt{-g} \left[\frac{M_{\text{pl}}^2}{2} R - \frac{1}{2} g^{\mu\nu} \partial_\mu \phi \partial_\nu \phi - V(\chi) \right]
\end{aligned} \tag{7}$$

where

$$\Omega^{-2}(x) = F'(\chi) = e^{\sqrt{\frac{2}{3}} \frac{\phi}{M_{\text{pl}}}}, \tag{8}$$

and the potential

$$V(\chi) = \frac{M_{\text{pl}}^2}{2} \left[\frac{\chi}{F'(\chi)} - \frac{F(\chi)}{F'(\chi)^2} \right]. \tag{9}$$

The first derivative of the potential with respect to χ is

$$\frac{dV(\chi)}{d\chi} = \left(\frac{M_{\text{pl}}^2}{2} \right) \frac{F''(\chi) [2F(\chi) - \chi F'(\chi)]}{F'(\chi)^3}. \tag{10}$$

Since $\frac{dV}{d\phi} = \frac{dV}{d\chi} \frac{d\chi}{d\phi}$ and

$$\frac{d\chi}{d\phi} = \sqrt{\frac{2}{3}} \frac{1}{M_{\text{pl}}} \frac{F'(\chi)}{F''(\chi)}, \tag{11}$$

we have

$$\frac{dV}{d\phi} = \frac{M_{\text{pl}}}{\sqrt{6}} \frac{2F(\chi) - \chi F'(\chi)}{F'(\chi)^2}, \tag{12}$$

and R and F in terms of the potential V

$$\begin{aligned}
R &= \left(\frac{\sqrt{6}}{M_{\text{pl}}} \frac{dV}{d\phi} + \frac{4V}{M_{\text{pl}}^2} \right) e^{\sqrt{\frac{2}{3}} \frac{\phi}{M_{\text{pl}}}}, \\
F &= \left(\frac{\sqrt{6}}{M_{\text{pl}}} \frac{dV}{d\phi} + \frac{2V}{M_{\text{pl}}^2} \right) e^{2\sqrt{\frac{2}{3}} \frac{\phi}{M_{\text{pl}}}}.
\end{aligned} \tag{13}$$

We adopt the Friedmann-Robertson-Walker (FRW) universe with the metric

$$ds^2 = -dt^2 + a(t)^2 d\mathbf{x}^2 = -dt^2 + a(t)^2 (dx^2 + dy^2 + dz^2), \quad (14)$$

where $a = a(t)$ is the scale factor and t is the cosmic time. Since the Einstein equation in the Einstein frame is given by

$$R_{\mu\nu} - \frac{1}{2}g_{\mu\nu}R = \frac{1}{M_{\text{pl}}^2}T_{\mu\nu}, \quad (15)$$

where $T_{\mu\nu}$ is the energy-momentum tensor in the Einstein frame given by

$$T_{\mu\nu} = \partial_\mu\phi\partial_\nu\phi - g_{\mu\nu}\left[\frac{1}{2}\partial^\sigma\phi\partial_\sigma\phi + V(\phi)\right], \quad (16)$$

if we take homogeneous scalar field $\phi(t, \mathbf{x}) = \phi(t)$, the equation of motion of the scalar field (inflaton field) in the Einstein frame is

$$\ddot{\phi}(t) + 3H\dot{\phi}(t) + V'(\phi) = 0, \quad (17)$$

and the 00 and ij components of the Einstein equation in the Einstein frame are given by

$$\begin{aligned} 3M_{\text{pl}}^2 H^2 &= \frac{1}{2}\dot{\phi}^2 + V(\phi), \\ \dot{H} &= -\frac{1}{2M_{\text{pl}}^2}\dot{\phi}^2, \end{aligned} \quad (18)$$

where $H(t) = \frac{\dot{a}(t)}{a(t)}$ is the Hubble parameter.

4 A Short Review: Starobinsky Model

$F(R)$ of the Starobinsky model is given by

$$F_{\text{Starobinsky}}(R) = R + 4g^2 R^2, \quad (19)$$

where $g \in \mathbb{R}^+$. After some algebra, we can obtain the potential in terms of inflaton field ϕ

$$V_{\text{Starobinsky}}(\phi) = \frac{M_{\text{pl}}^2}{32g^2} \left(1 - e^{-\sqrt{\frac{2}{3}}\frac{\phi}{M_{\text{pl}}}}\right)^2, \quad (20)$$

Originally, Starobinsky model was obtained by taking the lowest order of scalar curvature correction as in [10]. But in the recent years, there have been many motivations to obtain this model, one of which is $\mathcal{N} = 1$ SUGRA [34, 32]. In the following two subsections, we can see how the conformal SUGRA action can form the Starobinsky model, where the inflaton field comes from the lowest scalar component of a massive vector multiplet, and the dual of this action, where the bosonic part contains Starobinsky $F(R)$ term.

4.1 From the conformal SUGRA, ...

The conformal SUGRA action is given by [32, 34]

$$S = \left[\frac{1}{2} S_0 \bar{S}_0 \Phi (\Lambda + \bar{\Lambda} + g' V) \right] - \frac{1}{4} [\mathcal{W}^\alpha (V) \mathcal{W}_\alpha (V)]_F, \quad (21)$$

where S_0 is the chiral compensator, Λ is a Stueckelberg chiral multiplet, V is a vector multiplet, g' is the gauge coupling, $\Phi(x)$ is an arbitrary real function of x , \mathcal{W}^α is the field strength super-multiplet and $[\dots]_{D,F}$ are the super-conformal D and F term density formulae respectively [37]. After taking super-conformal gauge standard and integrating out all the auxiliary fields, we obtain the boson part of the Lagrangian in the Einstein frame as

$$\mathcal{L}_B = \sqrt{-g} \left[\frac{M_{\text{pl}}^2}{2} R - \frac{1}{4} \mathcal{F}_{\mu\nu} \mathcal{F}^{\mu\nu} - \frac{g'^2}{2} J'(C)^2 - \frac{1}{2} J''(C) \partial_\mu C \partial^\mu C - \frac{g'^2}{2} J''(C) \left(A_\mu - \frac{1}{g} \partial_\mu \theta \right)^2 \right], \quad (22)$$

where $C = \text{Re}\Lambda$, $\theta = \text{Im}\Lambda$ and Λ is a Stueckelberg chiral and the prime on J is the derivatives with respect to C , A_μ is the vector component of V , $F_{\mu\nu}$ is the field strength of A_μ and R denotes the Ricci scalar. Taking the $U(1)$ gauge as $\theta = 0$, $A_\mu = 0$ and $J = -\frac{3}{2} \ln(-\frac{1}{3} C e^C)$ and $\frac{\phi}{M_{\text{pl}}} = \sqrt{\frac{3}{2}} \ln(-C)$, the Lagrangian becomes

$$\mathcal{L}_B = \sqrt{-g} \left[\frac{M_{\text{pl}}^2}{2} R - \frac{1}{2} \partial_\mu \phi \partial^\mu \phi - \frac{9g'^2}{8} \left(1 - e^{-\sqrt{\frac{2}{3}} \frac{\phi}{M_{\text{pl}}}} \right)^2 \right], \quad (23)$$

which gives the Starobinsky model by taking $3g' = \frac{M_{\text{pl}}}{2g}$.

4.2 From the new minimal SUGRA, ...

The Starobinsky action in the new minimal SUGRA is given by [32, 34]

$$S_{\text{dual}} = \left[\frac{3}{2} L_0 V_R \right]_D - \gamma' [\mathcal{W}^\alpha (V_R) \mathcal{W}_\alpha (V_R)]_F. \quad (24)$$

where

$$V_R = \ln \left(\frac{L_0}{|\mathcal{S}|^2} \right) = \Lambda + \bar{\Lambda} + V, \quad (25)$$

is the dual transformation. \mathcal{S} is a chiral multiplet, V_R is a real multiplet, L_0 is a real linear compensator and γ' is a real constant. After taking this dual transformation, one can obtain the dual action

$$S_{\text{dual}} = \left[\frac{3}{2} L_0 V_R \right]_D - \gamma' [\mathcal{W}^\alpha (V) \mathcal{W}_\alpha (V)]_F. \quad (26)$$

After the field redefinition $\Lambda \rightarrow \Lambda/2$, $V \rightarrow g'V/2$, $\mathcal{S} \rightarrow S_0/\sqrt{3}$, we obtain

$$S_{\text{dual}} = \left[\frac{1}{2} |S_0|^2 \left(\frac{1}{2} (\Lambda + \bar{\Lambda} + g'V) \right) \exp \left(\frac{1}{2} (\Lambda + \bar{\Lambda} + g'V) \right) \right] - \frac{g'^2 \gamma'}{4} [\mathcal{W}^\alpha(V) \mathcal{W}_\alpha(V)]_F. \quad (27)$$

By taking $\gamma' = g'^{-2}$ and $\Phi(x) = xe^x$, we obtain Eq.(21). After the super-conformal gauge fixings, the bosonic part of the Lagrangian \mathcal{L} of Eq.(24) is

$$\frac{1}{\sqrt{-g}} \mathcal{L}|_B = \frac{M_{\text{pl}}^2}{2} R + \frac{M_{\text{pl}}^4 \gamma'}{18} R^2 - \gamma' \mathcal{F}_{\mu\nu}^{(R)} \mathcal{F}^{(R)\mu\nu} - \frac{3}{2} A_\mu^{(R)} B^\mu + \left(\frac{3}{4} + \frac{2\gamma'}{3} R \right) B_\mu B^\mu + \gamma' (B_\mu B^\mu)^2, \quad (28)$$

where $A_\mu^{(R)}$ is the vector component of V_R , $\mathcal{F}_{\mu\nu}^{(R)} = \partial_\mu A_\nu^{(R)} - \partial_\nu A_\mu^{(R)}$ and B_μ is an auxiliary vector component of L_0 . By taking $A_\mu^{(R)} = B_\mu = 0$, we obtain the Starobinsky $F(R)$ term $F(R) = R + M_{\text{pl}}^2 \gamma' R^2/9$ with an aid of $\gamma' = g'^{-2}$ and $3g' = \frac{M_{\text{pl}}}{2g}$.

5 The BI-extended model

Now we are going to consider BI-extended model

$$F_{\text{BI}}(R) = R + \frac{2g^2}{3\beta} \left(\sqrt{1 + 12\beta R^2} - 1 \right), \quad (29)$$

where⁷

$$g = \frac{1}{eM_{\text{pl}}}, \quad \text{and} \quad \beta = \frac{1}{e^2 M_{\text{BI}}^4} = \frac{g^2}{\alpha^4 M_{\text{pl}}^2}, \quad (30)$$

by defining $\alpha = \frac{M_{\text{BI}}}{M_{\text{pl}}}$. This model can be derived from DBI action of R^2 model in new minimal SUGRA, which is dual to DBI action of a massive vector multiplet. In the following two subsections, we are going to show this.

5.1 From DBI action of a massive vector multiplet, ...

The conformal SUGRA action is [33, 34]

$$S = \left[\frac{1}{2} |S_0|^2 \Phi(\Lambda + \bar{\Lambda} + g'V) \right]_D - [h S_0^3 X]_F \quad (31)$$

where

$$S_0^3 X = \mathcal{W}^\alpha \mathcal{W}_\alpha - X \Sigma_c(Q(\Lambda, \bar{\Lambda}) \bar{S}_0 \bar{X}), \quad (32)$$

where X is a chiral multiplet, $\Sigma_c(\cdot)$ is the chiral projection operator in conformal SUGRA, h is a real constant and $Q(\Lambda, \bar{\Lambda})$ is a real function of Λ and $\bar{\Lambda}$. After the super-conformal

⁷Based on the fact that $[F(R)] = M_{\text{pl}}^2$, we can know that the mass scales of R , β and g are $[R] = M_{\text{pl}}^2$, $[\beta] = M_{\text{pl}}^{-4}$ and $[g] = M_{\text{pl}}^{-1}$.

gauge fixings, integrating out all the auxiliary fields and choosing the $U(1)$ gauge condition $\theta = 0$ and taking $h = 1/4$ and $4M^4\omega = \exp(4J(C)/3)$, where M is a positive constant, we have the bosonic part of Lagrangian of Eq.(31)

$$\begin{aligned} \mathcal{L}|_B = \sqrt{-g} & \left[\frac{M_{\text{pl}}^2}{2} R - \frac{1}{2} J''(C) \partial_\mu C \partial^\mu C - \frac{g'^2}{2} J''(C) A_\mu A^\mu \right] \\ & + M^4 \left[1 - \sqrt{P} \sqrt{-\det \left(g_{\mu\nu} + \frac{1}{M^4} \mathcal{F}_{\mu\nu} \right)} \right], \end{aligned} \quad (33)$$

where

$$P = 1 + \frac{g'^2}{M^4} [J(C)]^2. \quad (34)$$

5.2 From DBI action of R^2 model in new minimal SUGRA, ...

The DBI action of new minimal $\mathcal{N} = 1$, $D = 4$ SUGRA consists of a real linear compensator L_0 , a real multiplet⁸ $V_R = \ln \left(\frac{L_0}{|\mathcal{S}|^2} \right)$ and a chiral multiplet \mathcal{S} . The action is given by [33, 34]

$$S_{\text{dual}} = \left[\frac{3}{2} L_0 V_R \right]_D + [-\gamma X(\mathcal{W}, \bar{\mathcal{W}}, L_0)]_F, \quad (35)$$

where γ is a real constant, and $X(\mathcal{W}, \bar{\mathcal{W}}, L_0)$ is a solution of the equation

$$X = \mathcal{W}^\alpha(V_R) \mathcal{W}_\alpha(V_R) - \kappa \Sigma_c(|X|^2 L_0^{-2}), \quad (36)$$

where κ is a positive constant. To solve X , we adopt the Lagrange multiplier multiplet \mathcal{M} as

$$S_{\text{dual}} = \left[\frac{3}{2} L_0 V_R \right]_D + [-\gamma X]_F + [2\mathcal{M}(\mathcal{W}^2(V_R) - \kappa \Sigma_c(|X|^2 L_0^{-2}) - X)]_F. \quad (37)$$

After the gauge fixing of V_R and the super-conformal symmetry, the bosonic part of the Lagrangian of Eq.(37) is given by

$$\begin{aligned} \mathcal{L}|_B = \sqrt{-g} & \left[\frac{M_{\text{pl}}^2}{2} R + \frac{3}{4} B_\mu B^\mu - \frac{3}{2} A_\mu^{(R)} B^\mu + 4\kappa (\text{Re}\mathcal{M}) |F^X|^2 - 4(\text{Re}\mathcal{M}) D_{(R)}^2 + 2(\text{Re}\mathcal{M}) \mathcal{F}_{\mu\nu}^{(R)} \mathcal{F}^{(R)\mu\nu} \right. \\ & \left. - 2i(\text{Im}\mathcal{M}) \mathcal{F}_{\mu\nu}^{(R)} \tilde{\mathcal{F}}^{(R)\mu\nu} - (\gamma + 2\mathcal{M}) F^X - (\gamma + 2\bar{\mathcal{M}}) \bar{F}^{\bar{X}} \right], \end{aligned} \quad (38)$$

where F^X is the F - term of X , $D_{(R)} := \frac{1}{3} \left(M_{\text{pl}}^2 R + \frac{3}{2} B_\mu B^\mu \right)$, $A_\mu^{(R)}$ is the vector component of V_R , B_μ is an auxiliary vector component of L_0 , and $\mathcal{F}_{\mu\nu}^{(R)} = \partial_\mu A_\nu^{(R)} - \partial_\nu A_\mu^{(R)}$.

⁸The dual transformation is the same as that of Starobinsky case.

After finding the equations of motion (E.O.M.)s of F^X , $\text{Re}\mathcal{M}$ and $\text{Im}\mathcal{M}$ and integrating out all of them, we obtain the on-shell action as follows

$$\mathcal{L}|_B = \sqrt{-g} \left[\frac{M_{\text{pl}}^2}{2} R + \frac{3}{4} B_\mu B^\mu - \frac{3}{2} A_\mu^{(R)} B^\mu - \frac{\gamma}{\kappa} + \frac{\gamma}{\kappa} \sqrt{4\kappa D_{(R)}^2 - \det(\eta_{ab} + \sqrt{\kappa} \mathcal{F}_{ab})} \right]. \quad (39)$$

The Lagrangian Eq.(39) has the DBI structure to the vector $A_\mu^{(R)}$. But surprisingly, it also includes the curvature scalar inside the square root, which contributes to the high order correction. By taking $A_\mu^{(R)} = B_\mu = 0$, we obtain

$$\mathcal{L}|_B = \sqrt{-g} \frac{M_{\text{pl}}^2}{2} \left[R + \frac{2g^2}{3\beta} \left(\sqrt{1 + 12\beta R^2} - 1 \right) \right], \quad (40)$$

which gives BI-extended $F(R)$ term $F_{\text{BI}}(R) = R + \frac{2g^2}{3\beta} \left(\sqrt{1 + 12\beta R^2} - 1 \right)$. [34] assumes the lowest scalar component of a vector multiplet is the inflaton field, while [35] assumes the inflaton field comes from scalar curvature via tensor scalar transformation. This paper assumes the inflaton field coming from scalar curvature instead of the lowest scalar component of a vector multiplet.

5.3 BI-extended Potential

To find the relationship between R and ϕ , by $F'(R) = e^{\sqrt{\frac{2}{3}} \frac{\phi}{M_{\text{pl}}}}$, we have

$$F'_{\text{BI}}(R) = 1 + \frac{8g^2 R}{\sqrt{1 + 12\beta R^2}} = e^{\sqrt{\frac{2}{3}} \frac{\phi}{M_{\text{pl}}}} \quad (41)$$

and on simplification we obtain

$$R^2 = \frac{\left(e^{\sqrt{\frac{2}{3}} \frac{\phi}{M_{\text{pl}}}} - 1 \right)^2}{64g^4 - 12\beta \left(e^{\sqrt{\frac{2}{3}} \frac{\phi}{M_{\text{pl}}}} - 1 \right)^2} \Rightarrow R = \frac{\pm \left(e^{\sqrt{\frac{2}{3}} \frac{\phi}{M_{\text{pl}}}} - 1 \right)}{\sqrt{64g^4 - 12\beta \left(e^{\sqrt{\frac{2}{3}} \frac{\phi}{M_{\text{pl}}}} - 1 \right)^2}}, \quad (42)$$

Since R is real, $R^2 \geq 0$, which implies⁹

$$\frac{16g^4}{3\beta} \geq \left(e^{\sqrt{\frac{2}{3}} \frac{\phi}{M_{\text{pl}}}} - 1 \right)^2 \Rightarrow 1 - \sqrt{\frac{16g^4}{3\beta}} \leq e^{\sqrt{\frac{2}{3}} \frac{\phi}{M_{\text{pl}}}} \leq 1 + \sqrt{\frac{16g^4}{3\beta}}. \quad (43)$$

⁹Note that $\beta > 0$. So, the inequality sign remains unchanged.

Also, from the physical point of view, since inflation occurred in dS spacetime, which has $R \geq 0$, and positive inflaton field value $\phi \geq 0$, and R is a smooth function of ϕ , it is physical to take

$$R = \frac{\left(e^{\sqrt{\frac{2}{3}} \frac{\phi}{M_{\text{pl}}}} - 1\right)}{\sqrt{64g^4 - 12\beta \left(e^{\sqrt{\frac{2}{3}} \frac{\phi}{M_{\text{pl}}}} - 1\right)^2}}, \quad (44)$$

where the denominator satisfies the criterion stated in Eq.(43). Since $\chi = R$ in the Legendre transformation and the potential is given by

$$V_{\text{BI}}(\chi) = \left(\frac{M_{\text{pl}}^2}{2}\right) \frac{\chi F'(\chi) - F(\chi)}{F'(\chi)^2} = \frac{g^2 \sqrt{12\beta\chi^2 + 1} \left(\sqrt{12\beta\chi^2 + 1} - 1\right) M_{\text{pl}}^2}{3\beta \left(\sqrt{12\beta\chi^2 + 1} + 8g^2\chi\right)^2}, \quad (45)$$

substituting Eq.(44) into Eq.(45), we obtain the BI-extended potential in terms of the inflaton field ϕ as

$$V_{\text{BI}}(\phi) = \frac{M_{\text{pl}}^2}{12\beta} e^{-2\sqrt{\frac{2}{3}} \frac{\phi}{M_{\text{pl}}}} \left\{ 4g^2 - \sqrt{16g^4 - 3\beta \left(e^{\sqrt{\frac{2}{3}} \frac{\phi}{M_{\text{pl}}}} - 1\right)^2} \right\}. \quad (46)$$

6 Numerical Calculation

6.1 Starobinsky model

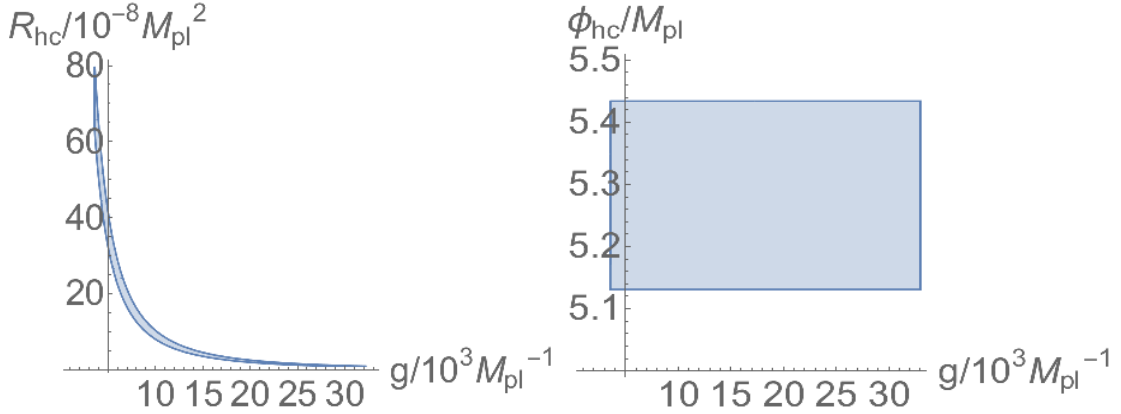


Figure 1: Left: g and R_{hc} based on the constraints listed in Table 1. Right: g and ϕ_{hc} based on the constraints listed in Table 1.

Based on Planck 2018 data constraints [7] listed in Table 1, we plot the region of possible values of g , scalar curvature at the first horizon crossing $R_{\text{hc}}/M_{\text{pl}}^2$ and initial inflaton field value¹⁰ $\phi_{\text{hc}}/M_{\text{pl}}$ as shown in Figure 1. We can see the scalar curvature at the horizon crossing is roughly inversely proportional to g , even though its scale is about $O(10^{-7}) M_{\text{pl}}^2$. The inflaton values at the first horizon crossing range from about $5.13M_{\text{pl}}$ to $5.44M_{\text{pl}}$ for all values of g greater than $3500M_{\text{pl}}^{-1}$. This range of g implies that the mass scale m given by $m^{-2} = 24g^2$ has a range¹¹ of $0 < m < 5.83212 \times 10^{-5} M_{\text{pl}}$.

6.2 BI-extended model

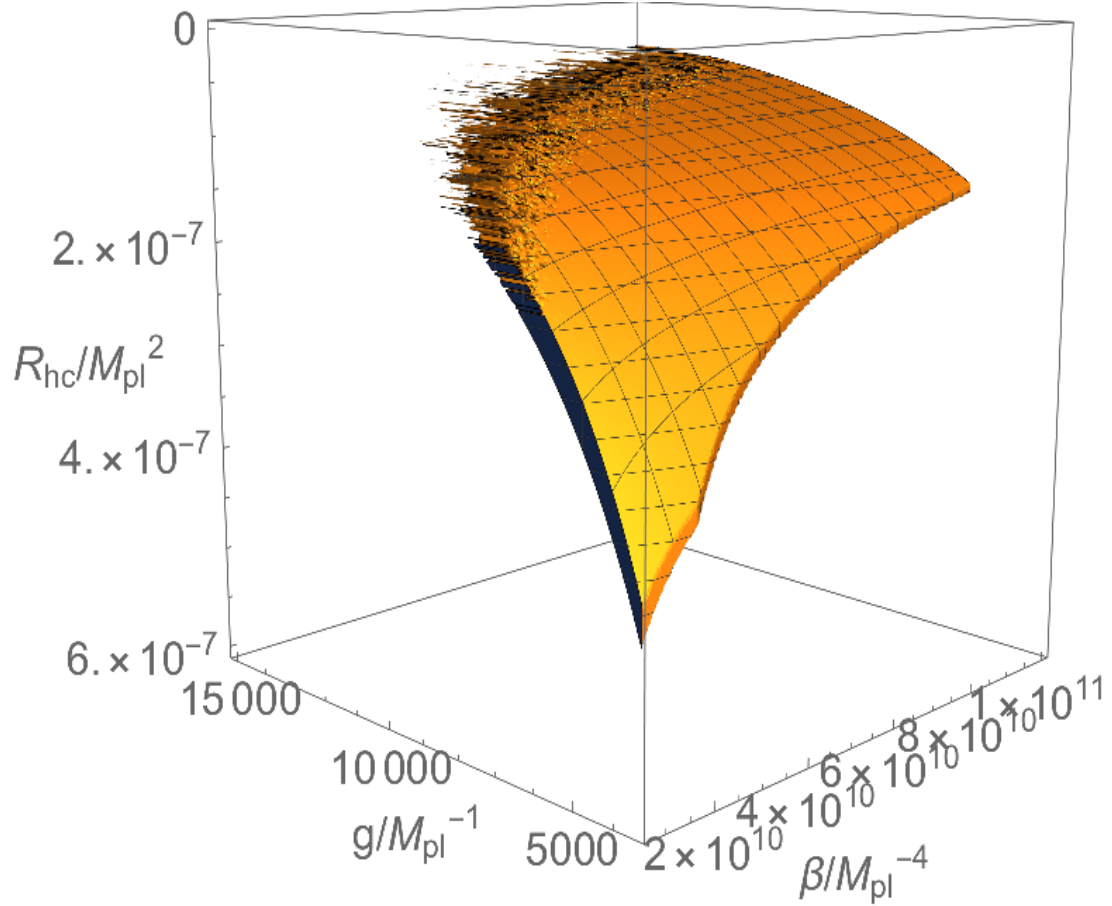


Figure 2: g , β and R_{hc} based on the constraints listed in Table 1. (Please pay attention to the magnitude direction of each axis.)

¹⁰ In this paper, the beginning of inflation is assumed to be the first horizon crossing.

¹¹Mathematically, it can be written as $-5.83212 \times 10^{-5} M_{\text{pl}} < m < 5.83212 \times 10^{-5} M_{\text{pl}}$. Given that m is positive, we remove the negative side.

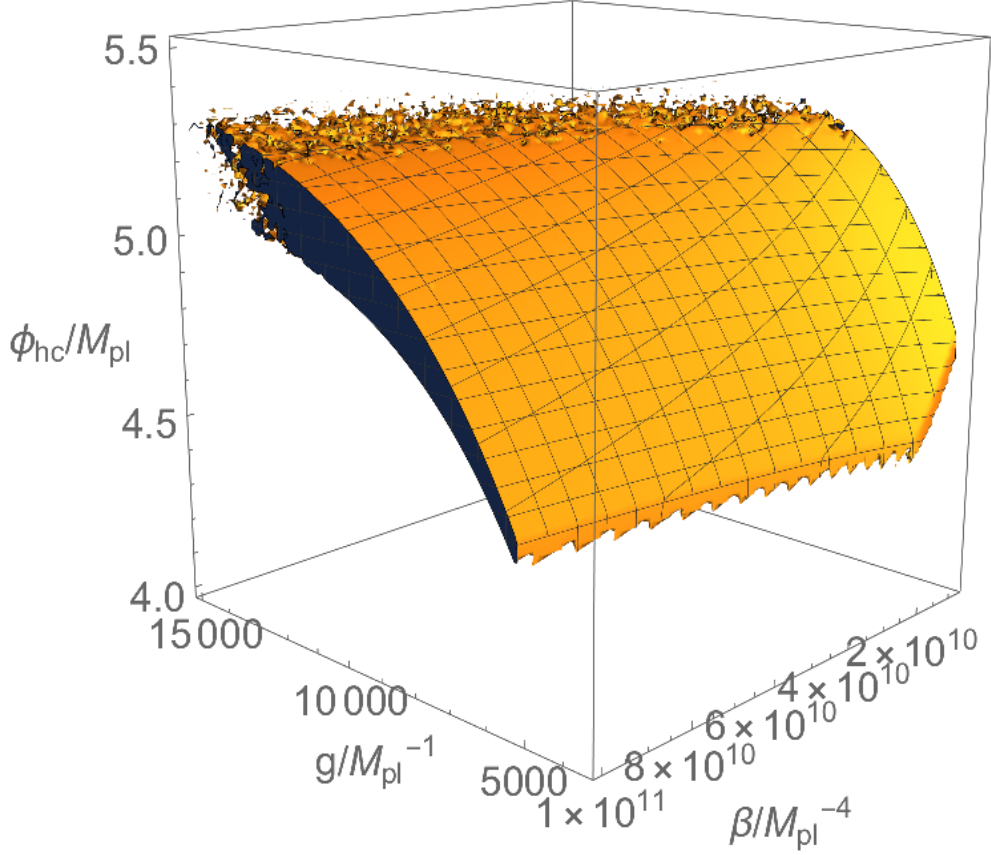


Figure 3: g , β and ϕ_{hc} based on the constraints listed in Table 1 for $10^{10} \leq \beta M_{pl}^4 \leq 10^{11}$. (Please pay attention to the magnitude direction of each axis.)

Based on Planck 2018 data constraints [7] listed in Table 1, we plot the region of possible values of g , β , scalar curvature and inflaton field value at the horizon crossing ϕ_{hc}/M_{pl} as shown in Figure 2, 3 and 4.¹² In fact, we can see the scalar curvature at the first horizon crossing is also roughly inversely proportional to g , even though its scale is about $O(10^{-7}) M_{pl}^2$. The inflaton values at the first horizon crossing range from about

¹²In previous work as shown in [2], inflaton values at the first horizon crossing are evaluated by obtaining the inflaton values at the end of inflation ϕ_{end} based on the condition of the end of inflation ($\epsilon_V(\phi_{end}) = 1$ or $\eta_V(\phi_{end}) = 1$), and the slow-roll approximation of e-folding formula $\Delta N = \int_{\phi_{hc}}^{\phi_{end}} H dt$. But, in this paper, we find the inflaton values at the first horizon crossing based on the observation data as shown in Table 1, and then verify the consistency of e-folding number (should be between 50 and 60 e-folds) based on those obtained inflaton values at the first horizon crossing and the exact e-folding formula $\Delta N = \int_{\phi_{hc}}^{\phi_{end}} H dt$ as shown in Table 2.

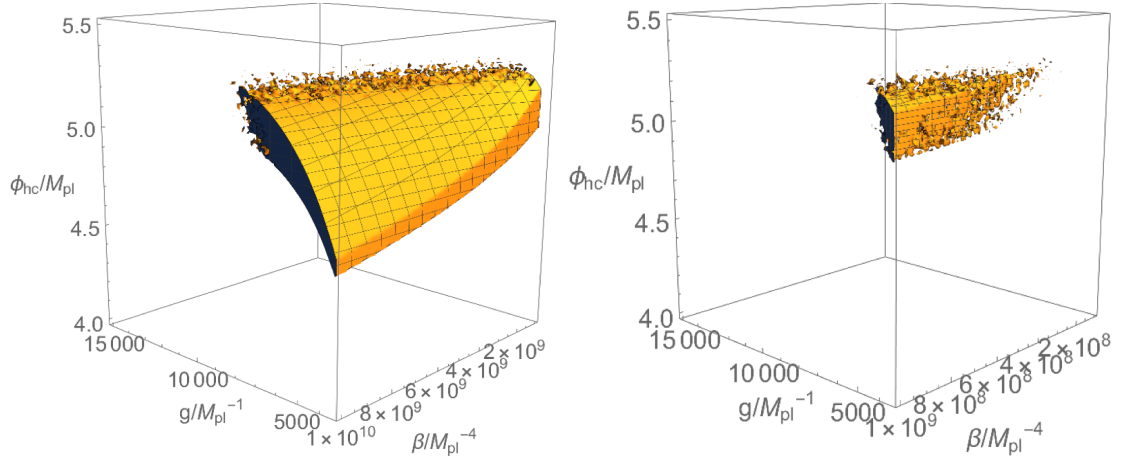


Figure 4: Left: g , β and ϕ_{hc} based on the constraints listed in Table 1 for $10^9 \leq \beta M_{\text{pl}}^4 \leq 10^{10}$. Right: Same for $10^8 \leq \beta M_{\text{pl}}^4 \leq 10^9$. (Please pay attention to the magnitude direction of each axis.)

$4.7M_{\text{pl}}$ to $5.2M_{\text{pl}}$ depending on some particular values of g greater than $5000M_{\text{pl}}^{-1}$, while β is greater than $O(10^8)M_{\text{pl}}^{-4}$. Apart from this, we plot the possible values of e and α in Fig. 5 by the constraints in Table 1 and Eq.(30). The upper possible limits of e and α are

$$e \leq 2.8 \times 10^{-4}, \quad \text{and} \quad \alpha \leq 0.41. \quad (47)$$

6.3 Potential graph under variations of g and β

In this subsection, we are going to discuss the shapes of the BI-extended potential and the fingerprints in the $n_s - r$ graph when g and β vary. First, we can see that even though BI-extended potential Eq. (46) has a similar shape with that of Starobinsky potential Eq. (20) during the inflation as shown in Fig.(6). BI-extended potential has a higher value to start the inflation as g decreases. It also has the "tail" at a larger inflaton field value as β decreases. The tip of each tail ceases according to the real curvature criterion Eq. (43).

6.4 $n_s - r$ graph under variations of g and β

Variations of g and β give various fingerprints in the graph of the tensor-to-scalar ratio r against the scalar spectral index n_s as shown in Fig.(7). With the reference points of Starobinsky model shown as blue points, BI-extended model gives the fingerprints tending to those blue points as g increases. BI-extended fingerprints start from $\beta = 10^{10}M_{\text{pl}}^{-4}$ and $\beta = 2 \times 10^{10}M_{\text{pl}}^{-4}$ at triangle and square points respectively. This implies that BI-extended fingerprints are away from the observation data as β increases.

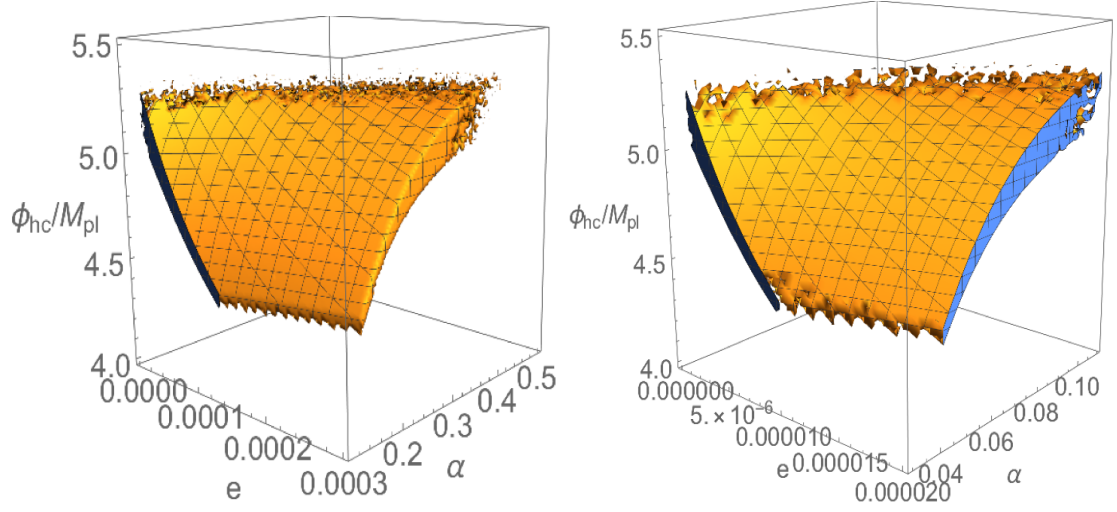


Figure 5: Left: e , α and ϕ_{hc} based on the constraints listed in Table 1 for the ranges $10^{-5} \leq e \leq 3 \times 10^{-4}$ and $0.11 \leq \alpha \leq 0.5$. Right: Same for the ranges $10^{-9} \leq e \leq 2 \times 10^{-5}$ and $0.03 \leq \alpha \leq 0.11$. (Please pay attention to the magnitude direction and the scale of each axis.)

7 Evolutions of inflaton field

Color, style	Model	$g/10^3 M_{\text{pl}}^{-1}$	$\beta/10^{10} M_{\text{pl}}^{-4}$	$t/M_{\text{pl}}^{-1}(N = 50)$	$t/M_{\text{pl}}^{-1}(N = 60)$
Red, Thick	BI	10	2	5.069835×10^6	$> 3.985 \times 10^7$
Green, Thick	BI	9.5	2	4.817745×10^6	$> 5.098 \times 10^7$
Blue, Thick	BI	9	2	4.565945×10^6	$> 5.708 \times 10^7$
Black, Thick	BI	8.5	2	4.314575×10^6	$> 6.314 \times 10^7$
Gray, Thick	BI	8	2	4.063815×10^6	$> 6.726 \times 10^7$
Red, Dashed(tiny)	BI	10	1	5.0667135×10^6	$> 5.052 \times 10^7$
Green, Dashed(tiny)	BI	9.5	1	4.814035×10^6	$> 6.094 \times 10^7$
Blue, Dashed(tiny)	BI	9	1	4.561495×10^6	$> 7.117 \times 10^7$
Black, Dashed(tiny)	BI	8.5	1	4.309125×10^6	$> 8.233 \times 10^7$
Gray, Dashed(tiny)	BI	8	1	4.057005×10^6	$> 9.216 \times 10^7$
Red, Dashed(long)	Staro	10	N/A	5.06373×10^6	$> 3.962 \times 10^7$
Green, Dashed(long)	Staro	9.5	N/A	4.810548×10^6	$> 4.933 \times 10^7$
Blue, Dashed(long)	Staro	9	N/A	4.557355×10^6	$> 5.273 \times 10^7$
Black, Dashed(long)	Staro	8.5	N/A	4.304175×10^6	$> 5.422 \times 10^7$
Gray, Dashed(long)	Staro	8	N/A	4.050985×10^6	$> 5.934 \times 10^7$

Table 2: Inflaton field evolution data starting from $\phi = 5.3 M_{\text{pl}}$ and $\dot{\phi}(t = 0) = 0$. The pairs of color and style can be referred to the plot legend in Fig.(6).

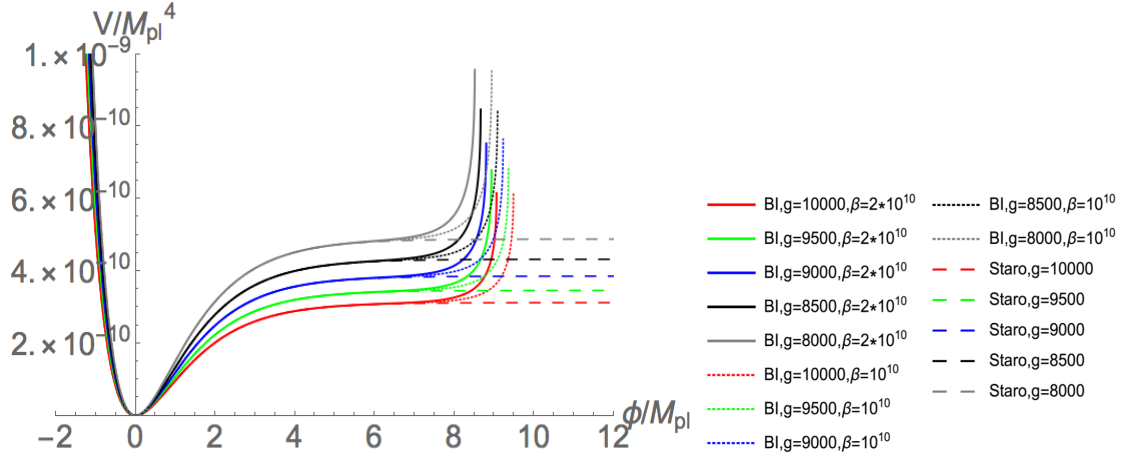


Figure 6: Left: This graph shows the potential against inflaton field values. The solid, tiny dashed and large dashed lines describe the BI-extended potential at $\beta = 2 \times 10^{10} M_{\text{pl}}^{-4}$, the counterpart at $\beta = 10^{10} M_{\text{pl}}^{-4}$ and the Starobinsky potential respectively. Around $\phi = 6 M_{\text{pl}}$, the potential lines are plotted from $g = 8000 M_{\text{pl}}^{-1}$ on the top to $g = 10000 M_{\text{pl}}^{-1}$ on the bottom.) Since the universe started the inflation from about $5.1 - 5.4 M_{\text{pl}}$ as shown in Figure 1 and Figure 3, the universe has a higher initial potential scale as g decreases. The universe rolled down to the trough at some inflaton value(s) such that either slow roll parameters ϵ or η became close to 1 as the end of inflation. Right: The plot legend. "BI" means BI-extended model while "Staro" means the Starobinsky model.

In this part, we are going to investigate how the inflaton field evolves as (g, β) vary. First of all, we are going to find the initial rate of change of inflaton field $\dot{\phi}(t)$. By adopting the Friedman equation in Eq.(18) and the constraints in Table 1 as demonstrated in [36], we obtain the region plot in Fig.(8). We can see that the region is enclosed by a parabolic curve with the x-axis since the speed of inflaton field $\dot{\phi}(t)$ (x -axis) is parabolic in the Friedman equation while the potential (y -axis) is linear. We can also understand that $\dot{\phi}(t=0)$ ranges from $-6 \times 10^{-5} M_{\text{pl}}^2$ to $6 \times 10^{-5} M_{\text{pl}}^2$ while V_{hc} ranges from 0 to $2.2 \times 10^{-9} M_{\text{pl}}^4$.

Apart from this, we plot time evolutions of $\phi(t)/M_{\text{pl}}$ and $H(t)/M_{\text{pl}}$ with initial conditions $\phi(t=0) = 5.3 M_{\text{pl}}$ and $\dot{\phi}(t=0) = 0$ under variations of g and β in Fig.(8) and Fig.(9) respectively. In Fig.(8), one can see that all colors of $\phi(t)$ decay continuously from $5.3 M_{\text{pl}}$ to $0.5 M_{\text{pl}}$ and then oscillate around 0. The evolutions carry out oscillations earlier for larger g and β . On the other hand, in Fig.(9), one can see that even though different colors start from various initial Hubble values, all colors of $H(t)$ remain constant from $t = 0$ to $t = 4 \times 10^6 M_{\text{pl}}^{-1}$, and then start to decay to approach 0 between $t = 4 \times 10^6 M_{\text{pl}}^{-1}$ and $t = 6 \times 10^6 M_{\text{pl}}^{-1}$. This verifies that the initial stage of inflation can

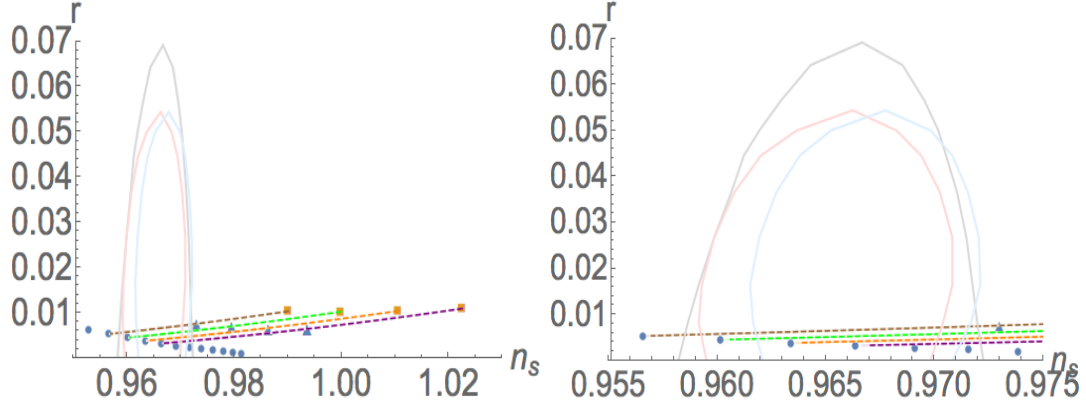


Figure 7: Left: The tensor-to-scalar ratio r against the scalar spectral index n_s are plotted as above. The light color lines represent the boundaries of the observation data of 68 % CL in Planck 2018 (Light gray for TT,TE,EE+lowE+lensing, light red for TT,TE,EE+lowE+lensing+BK14 and light blue for TT,TE,EE+lowE+lensing+BK14+BAO). The blue dots represent the fingerprints of Starobinsky model, from the inflaton values at the first horizon crossing $\phi_{\text{hc}} = 5 M_{\text{pl}}$ on the left to $\phi_{\text{hc}} = 6.1 M_{\text{pl}}$ on the right with a spacing of $0.1 M_{\text{pl}}$. The square points represent the fingerprints of BI-extended model at $g = 5000 M_{\text{pl}}^{-1}$ and $\beta = 2 \times 10^{10} M_{\text{pl}}^{-4}$ while the triangle points represent the counterparts at $g = 5000 M_{\text{pl}}^{-1}$ and $\beta = 10^{10} M_{\text{pl}}^{-4}$. The brown, green, orange and purple dashed lines represent $\phi_{\text{hc}} = 5.1 M_{\text{pl}}$, $5.2 M_{\text{pl}}$, $5.3 M_{\text{pl}}$, $5.4 M_{\text{pl}}$ respectively. As g increases from $5000 M_{\text{pl}}^{-1}$ to $15000 M_{\text{pl}}^{-1}$, they go along the corresponding dashed lines towards the blue points (Starobinsky fingerprints) from the corresponding square and triangle points respectively. Right: This graph focuses on the inner observation regions.

be approximated as "quasi-static"¹³. The evolutions decay earlier for larger g and β as well.

8 Discussions

Basically, from the potential graph shown in Fig.(6), we can understand that the inflation processes described by BI-extended and Starobinsky models are similar, even though their shapes are different in the regions out of inflation dynamics. We can also know that the feasible scales of BI-extended model are $g \approx O(10^3) M_{\text{pl}}^{-1}$ and $\beta \approx O(10^8) M_{\text{pl}}^{-4}$. Since the scale of the scalar curvature at the first horizon crossing is given by $R \approx O(10^{-7}) M_{\text{pl}}^2$, by Eq. (29), we know that the total scale of $12\beta R^2$ becomes about $O(10^{-4})$, which is much less than 1. The square root function in Eq. (29) can be well approximated as

¹³The words "quasi static" means the Hubble parameter $H(t)$ is constant.

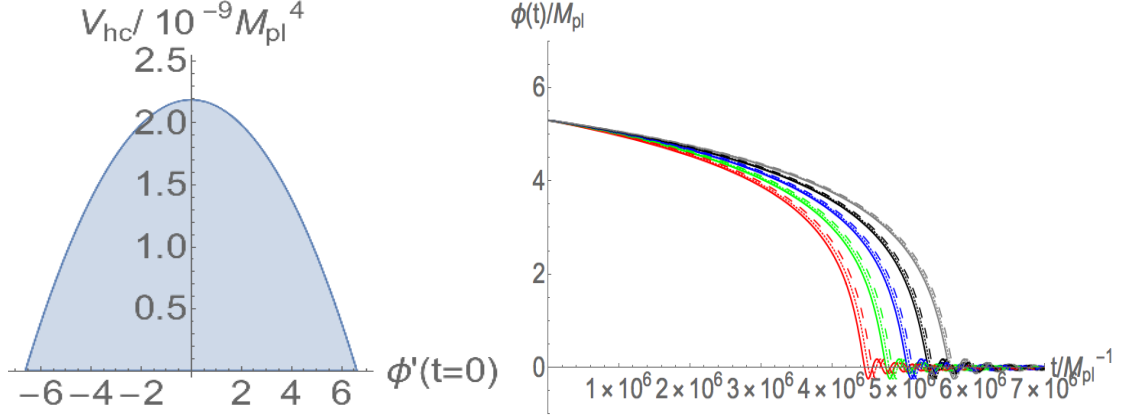


Figure 8: Left: These region plots show the potential scale against the speed of inflaton field at the first horizon crossing based on Table 1. The horizontal axis (x -axis) and the vertical axis (y -axis) represent the speed of inflaton field $\dot{\phi}(t)/10^{-5}M_{\text{pl}}^2$ and the potential scale $V(\phi)/10^{-9}M_{\text{pl}}^4$ (at the first horizon crossing) respectively. Right: This graph shows the time evolution of inflaton field with respect to cosmic time t . The colors can be referred to the plot legend in Fig.(6).

$\sqrt{1 + 12\beta R^2} \approx 1 + 6\beta R^2$, which reduces BI-extended model to the Starobinsky counterpart. Since the inflaton value decreases from about $5.3M_{\text{pl}}$ to about $1M_{\text{pl}}$ during inflation process, by Eq.(42), the (positive) value of scalar curvature decreases, which keeps the approximation of the square root function valid.

Apart from this, in Fig.(6), there are sharply increasing "tails" in BI-extended potentials as ϕ increases, and then stop at some certain values. In fact, as ϕ increases, $e^{\sqrt{\frac{2}{3}}\frac{\phi}{M_{\text{pl}}}}$ in Eq.(46) also increases significantly, resulting in a decline of $16g^4 - 3\beta \left(e^{\sqrt{\frac{2}{3}}\frac{\phi}{M_{\text{pl}}}} - 1 \right)^2$ from a positive value to 0, at which the curvature criterion Eq.(43) takes effect. On the other side, as ϕ decreases to negative values through 0, the exponential factor $e^{\sqrt{\frac{2}{3}}\frac{\phi}{M_{\text{pl}}}}$ declines and approaches to 0, leading to a constant value for $16g^4 - 3\beta \left(e^{\sqrt{\frac{2}{3}}\frac{\phi}{M_{\text{pl}}}} - 1 \right)^2$.

However, the factor $e^{-2\sqrt{\frac{2}{3}}\frac{\phi}{M_{\text{pl}}}}$ rises dramatically to approach infinity, causing surges of BI-extended potentials.

In addition, even though the variations of (g, β) of BI-extended models on (n_s, r) are along their corresponding dashed lines, from Fig.(7) we can understand that observations favor

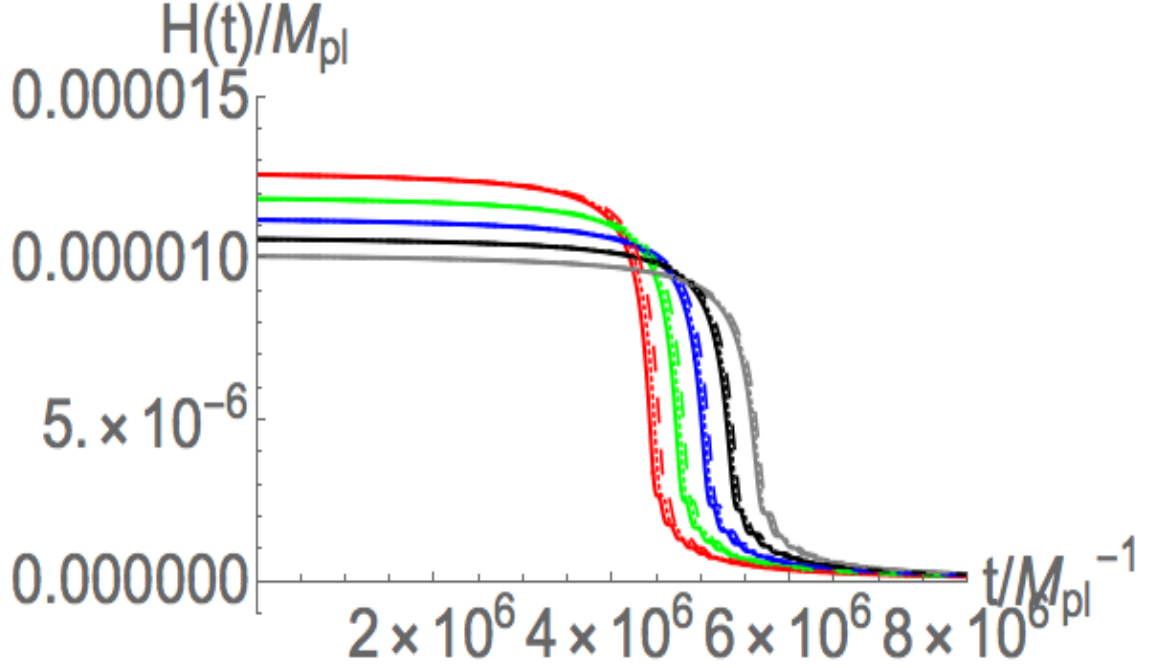


Figure 9: This graph shows the time evolution of the Hubble parameter with respect to cosmic time t . The colors can be referred to the plot legend in Fig.(6).

large g and small β . BI-extended models also agree with the inflaton values at the first horizon crossing ranging from $5.1M_{\text{pl}}$ to $5.4M_{\text{pl}}$, which have the same value tolerance as that of Starobinsky potential at the first horizon crossing. Since BI-extended model gives nearly the same effective inflation dynamics as Starobinsky model, further investigation is required to verify which one, BI-extended or Starobinsky model, is the correct model for describing the beginning of inflation. It is also meaningful to find the theoretical reasons why observation data favor large g and small β in BI-extended model. Nevertheless, BI-extended model can be one of the extensions of Starobinsky model for describing the inflation dynamics at the first horizon crossing, and the high order terms can refine the prediction of original Starobinsky model.

9 Conclusions

To conclude, we analyze BI-extended model in a complete form and compare the predictions with that of Starobinsky model. Under the observation constraints of Planck 2018, we find that the inflation processes described by BI-extended and Starobinsky models are nearly the same. The required scales of g and β are approximately at least $O(10^3) M_{\text{pl}}^{-1}$ and $O(10^8) M_{\text{pl}}^{-4}$ respectively, which give the upper limit of the coupling e and the ratio

of M_{BI} to M_{pl} as $e \leq 2.8 \times 10^{-4}$ and $\alpha \leq 0.41$ respectively. Furthermore, we investigate the changes of predictions of (n_s, r) and the evolutions of inflaton field under the variations of (g, β) . BI-extended model can be one of the extensions of Starobinsky model for high energy scale.

10 Acknowledgements

The author thanks Prof. Hiroyuki ABE very much for suggestion and useful discussions. The author is supported by Waseda University Scholarship.

A Appendix: Potential and its derivatives

In this section, we are going to discuss the full derivation of the potential and its derivatives for slow-roll parameters. Given that the derivative of χ with respect to ϕ is given by

$$\frac{d\chi}{d\phi} = \frac{1}{M_{\text{pl}}} \sqrt{\frac{2}{3}} \frac{F'(\chi)}{F''(\chi)}, \quad (48)$$

its first derivative with respect to χ is given by

$$\frac{d}{d\chi} \left(\frac{d\chi}{d\phi} \right) = \frac{1}{M_{\text{pl}}} \sqrt{\frac{2}{3}} \frac{[F''(\chi)^2 - F^{(3)}(\chi)F'(\chi)]}{F''(\chi)^2}. \quad (49)$$

Its second derivative with respect to χ is given by

$$\frac{d^2}{d\chi^2} \left(\frac{d\chi}{d\phi} \right) = \frac{-1}{M_{\text{pl}}} \sqrt{\frac{2}{3}} \frac{[F^{(3)}(\chi)F''(\chi)^2 - 2F^{(3)}(\chi)^2F'(\chi) + F^{(4)}(\chi)F'(\chi)F''(\chi)]}{F''(\chi)^3}. \quad (50)$$

Its third derivative with respect to χ is given by

$$\begin{aligned} \frac{d^3}{d\chi^3} \left(\frac{d\chi}{d\phi} \right) = & \frac{-1}{M_{\text{pl}}} \sqrt{\frac{2}{3}} \frac{1}{F''(\chi)^4} \left[2F^{(4)}(\chi)F''(\chi)^3 + 6F^{(3)}(\chi)^3F'(\chi) \right. \\ & \left. + \left(F^{(5)}(\chi)F'(\chi) - 3F^{(3)}(\chi)^2 \right) F''(\chi)^2 - 6F^{(3)}(\chi)F^{(4)}(\chi)F'(\chi)F''(\chi) \right], \end{aligned} \quad (51)$$

where $F'(\chi)$, $F''(\chi)$, $F^{(3)}(\chi)$ and $F^{(4)}(\chi)$ are the first, second, third and fourth derivatives of $F(\chi)$ with respect to χ respectively. The potential is given by

$$V(\chi) = \left(\frac{M_{\text{pl}}^2}{2} \right) \frac{\chi F'(\chi) - F(\chi)}{F'(\chi)^2}, \quad (52)$$

and its first, second and third derivatives with respect to χ are given by

$$V'(\chi) = \left(\frac{M_{\text{pl}}^2}{2} \right) F''(\chi) \frac{2F(\chi) - \chi F'(\chi)}{F'(\chi)^3}, \quad (53)$$

$$V''(\chi) = \frac{M_{\text{pl}}^2}{2F'(\chi)^4} \left[-6F(\chi)F''(\chi)^2 + F'(\chi)^2 \left(F''(\chi) - \chi F^{(3)}(\chi) \right) + 2F'(\chi) \left(F(\chi)F^{(3)}(\chi) + \chi F''(\chi)^2 \right) \right], \quad (54)$$

$$V'''(\chi) = \frac{-M_{\text{pl}}^2}{2F'(\chi)^5} \left[-24F(\chi)F''(\chi)^3 + \left(\chi F^{(4)}(\chi) - 2F^{(3)}(\chi) \right) F'(\chi)^3 + 6F'(\chi) \left(\chi F''(\chi)^3 + 3F(\chi)F^{(3)}(\chi)F''(\chi) \right) + F'(\chi)^2 \left(-2F(\chi)F^{(4)}(\chi) + 6F''(\chi)^2 - 6\chi F^{(3)}(\chi)F''(\chi) \right) \right], \quad (55)$$

$$V''''(\chi) = \frac{-M_{\text{pl}}^2}{2F'(\chi)^6} \left[120F(\chi)F''(\chi)^4 + \left(\chi F^{(5)}(\chi) - 3F^{(4)}(\chi) \right) F'(\chi)^4 - 24F'(\chi) \left(\chi F''(\chi)^4 + 6F(\chi)F^{(3)}(\chi)F''(\chi)^2 \right) - 6F'(\chi)^2 \left(-3F(\chi)F^{(3)}(\chi)^2 + 6F''(\chi)^3 - 4F(\chi)F^{(4)}(\chi)F''(\chi) - 6\chi F^{(3)}(\chi)F''(\chi)^2 \right) - 2F'(\chi)^3 \left(F(\chi)F^{(5)}(\chi) + 3\chi F^{(3)}(\chi)^2 + \left(4\chi F^{(4)}(\chi) - 14F^{(3)}(\chi) \right) F''(\chi) \right) \right]. \quad (56)$$

The first, second, third and fourth derivatives of the potential with respect to ϕ are given by

$$\frac{dV}{d\phi} = V'(\chi) \frac{d\chi}{d\phi} = \frac{M_{\text{pl}}}{\sqrt{6}} \frac{2F - \chi F'}{F'^2}, \quad (57)$$

$$\begin{aligned} \frac{d^2V}{d\phi^2} &= V''(\chi) \left(\frac{d\chi}{d\phi} \right)^2 + V'(\chi) \frac{d\chi}{d\phi} \frac{d}{d\chi} \left(\frac{d\chi}{d\phi} \right) \\ &= \frac{1}{3} \left[\frac{1}{F''(\chi)} + \frac{\chi}{F'(\chi)} - \frac{4F(\chi)}{F'(\chi)^2} \right], \end{aligned} \quad (58)$$

$$\begin{aligned} \frac{d^3V}{d\phi^3} &= V^{(3)}(\chi) \left(\frac{d\chi}{d\phi} \right)^3 + 3V''(\chi) \left(\frac{d\chi}{d\phi} \right)^2 \frac{d}{d\chi} \left(\frac{d\chi}{d\phi} \right) + V'(\chi) \frac{d\chi}{d\phi} \left[\frac{d}{d\chi} \left(\frac{d\chi}{d\phi} \right) \right]^2 \\ &\quad + V'(\chi) \left(\frac{d\chi}{d\phi} \right)^2 \frac{d^2}{d\chi^2} \left(\frac{d\chi}{d\phi} \right) \\ &= \frac{-1}{3M_{\text{pl}}} \sqrt{\frac{2}{3}} \frac{1}{F'(\chi)^2 F''(\chi)^3} \left[-8F(\chi)F''(\chi)^3 + F^{(3)}(\chi)F'(\chi)^3 + 3F'(\chi)^2 F''(\chi)^2 + \chi F'(\chi)F''(\chi)^3 \right] \end{aligned} \quad (59)$$

$$\begin{aligned}
\frac{d^4 V}{d\phi^4} &= V^{(4)}(\chi) \left(\frac{d\chi}{d\phi} \right)^4 + 6V^{(3)}(\chi) \left(\frac{d\chi}{d\phi} \right)^3 \frac{d}{d\chi} \left(\frac{d\chi}{d\phi} \right) + 7V^{(2)}(\chi) \left(\frac{d\chi}{d\phi} \right)^2 \left[\frac{d}{d\chi} \left(\frac{d\chi}{d\phi} \right) \right]^2 \\
&\quad + 4V^{(2)}(\chi) \left(\frac{d\chi}{d\phi} \right)^3 \frac{d^2}{d\chi^2} \left(\frac{d\chi}{d\phi} \right) + 4V'(\chi) \left(\frac{d\chi}{d\phi} \right)^2 \left[\frac{d}{d\chi} \left(\frac{d\chi}{d\phi} \right) \right] \frac{d^2}{d\chi^2} \left(\frac{d\chi}{d\phi} \right) \\
&\quad + V'(\chi) \left(\frac{d\chi}{d\phi} \right)^3 \frac{d^3}{d\chi^3} \left(\frac{d\chi}{d\phi} \right) \\
&= \frac{-2}{9M_{\text{pl}}^2 F'(\chi)^2 F''(\chi)^6} \left[18F(\chi)F''(\chi)^6 - 2F'(\chi) \left(\chi F''(\chi)^6 + 3F(\chi)F^{(3)}(\chi)F''(\chi)^4 \right) \right. \\
&\quad - F^{(3)}(\chi)F'(\chi)^3 \left(2F(\chi)F^{(3)}(\chi)^2 + 2F''(\chi)^3 + 3\chi F^{(3)}(\chi)F''(\chi)^2 \right) \\
&\quad + F'(\chi)^2 \left(-7F''(\chi)^5 + 3\chi F^{(3)}(\chi)F''(\chi)^4 + 6F(\chi)F^{(3)}(\chi)^2 F''(\chi)^2 \right) \\
&\quad \left. + F'(\chi)^4 \left(\chi F^{(3)}(\chi)^3 + F^{(4)}(\chi)F''(\chi)^2 - 3F^{(3)}(\chi)^2 F''(\chi) \right) \right], \tag{60}
\end{aligned}$$

and the normalized derivatives are given by

$$\frac{1}{V} \frac{dV}{d\phi} = -\sqrt{\frac{2}{3}} \frac{1}{M_{\text{pl}}} \frac{\chi F' - 2F}{\chi F' - F}. \tag{61}$$

$$\frac{1}{V} \frac{d^2 V}{d\phi^2} = -\frac{2}{3M_{\text{pl}}^2} \frac{[-4F(\chi)F''(\chi) + F'(\chi)^2 + \chi F'(\chi)F''(\chi)]}{[F(\chi) - \chi F'(\chi)] F''(\chi)}. \tag{62}$$

$$\frac{1}{V} \frac{d^3 V}{d\phi^3} = \frac{1}{M_{\text{pl}}^3} \left(\frac{2}{3} \right)^{\frac{3}{2}} \frac{[-8F(\chi)F''(\chi)^3 + F^{(3)}(\chi)F'(\chi)^3 + 3F'(\chi)^2 F''(\chi)^2 + \chi F'(\chi)F''(\chi)^3]}{[F(\chi) - \chi F'(\chi)] F''(\chi)^3}, \tag{63}$$

$$\begin{aligned}
\frac{1}{V} \frac{d^4 V}{d\phi^4} &= \frac{4}{9M_{\text{pl}}^4 (F(\chi) - \chi F'(\chi)) F''(\chi)^6} \left[18F(\chi)F''(\chi)^6 \right. \\
&\quad - 2F'(\chi) \left(\chi F''(\chi)^6 + 3F(\chi)F^{(3)}(\chi)F''(\chi)^4 \right) \\
&\quad - F^{(3)}(\chi)F'(\chi)^3 \left(2F(\chi)F^{(3)}(\chi)^2 + 2F''(\chi)^3 + 3\chi F^{(3)}(\chi)F''(\chi)^2 \right) \\
&\quad + F'(\chi)^2 \left(-7F''(\chi)^5 + 3\chi F^{(3)}(\chi)F''(\chi)^4 + 6F(\chi)F^{(3)}(\chi)^2 F''(\chi)^2 \right) \\
&\quad \left. + F'(\chi)^4 \left(\chi F^{(3)}(\chi)^3 + F^{(4)}(\chi)F''(\chi)^2 - 3F^{(3)}(\chi)^2 F''(\chi) \right) \right]. \tag{64}
\end{aligned}$$

Based on the above derivatives, the slow roll parameters defined as

$$\begin{aligned}
\epsilon_V &\equiv \text{1st order} \equiv \frac{1}{2} M_{\text{pl}}^2 \left(\frac{V'(\phi)}{V(\phi)} \right)^2, \\
\eta_V &\equiv \text{2nd order} \equiv M_{\text{pl}}^2 \left(\frac{V''(\phi)}{V(\phi)} \right), \\
\xi_V &\equiv \text{3rd order} \equiv M_{\text{pl}}^4 \left(\frac{V'(\phi) V'''(\phi)}{V(\phi)^2} \right), \\
\omega_V &\equiv \text{4th order} \equiv M_{\text{pl}}^6 \left(\frac{V'(\phi)^2 V''''(\phi)}{V(\phi)^3} \right).
\end{aligned} \tag{65}$$

are given by

$$\epsilon_V = \frac{(\chi F'(\chi) - 2F(\chi))^2}{3(F(\chi) - \chi F'(\chi))^2}, \tag{66}$$

$$\eta_V = -\frac{2(-4F(\chi)F''(\chi) + F'(\chi)^2 + \chi F'(\chi)F''(\chi))}{3(F(\chi) - \chi F'(\chi))F''(\chi)}, \tag{67}$$

$$\begin{aligned}
\xi_V &= \frac{4(\chi F'(\chi) - 2F(\chi))}{9(F(\chi) - \chi F'(\chi))^2 F''(\chi)^3} \left[-8F(\chi)F''(\chi)^3 + F^{(3)}(\chi)F'(\chi)^3 \right. \\
&\quad \left. + 3F'(\chi)^2 F''(\chi)^2 + \chi F'(\chi)F''(\chi)^3 \right],
\end{aligned} \tag{68}$$

$$\begin{aligned}
\omega_V &= \frac{-8(\chi F'(\chi) - 2F(\chi))^2}{27(F(\chi) - \chi F'(\chi))^3 F''(\chi)^6} \left[-18F(\chi)F''(\chi)^6 \right. \\
&\quad + 2F'(\chi) \left(\chi F''(\chi)^6 + 3F(\chi)F^{(3)}(\chi)F''(\chi)^4 \right) \\
&\quad + F^{(3)}(\chi)F'(\chi)^3 \left(2F(\chi)F^{(3)}(\chi)^2 + 2F''(\chi)^3 + 3\chi F^{(3)}(\chi)F''(\chi)^2 \right) \\
&\quad + F'(\chi)^2 \left(7F''(\chi)^5 - 3\chi F^{(3)}(\chi)F''(\chi)^4 - 6F(\chi)F^{(3)}(\chi)^2 F''(\chi)^2 \right) \\
&\quad \left. - F'(\chi)^4 \left(\chi F^{(3)}(\chi)^3 + F^{(4)}(\chi)F''(\chi)^2 - 3F^{(3)}(\chi)^2 F''(\chi) \right) \right].
\end{aligned} \tag{69}$$

Then, we can obtain the scalar spectral index n_s and its running¹⁴

$$\begin{aligned}
n_s &\simeq 1 + 2\eta_V - 6\epsilon_V \\
&= \frac{-5F(\chi)^2 F''(\chi) - 2F(\chi)F'(\chi)(\chi F''(\chi) + 2F'(\chi)) + \chi F'(\chi)^2(\chi F''(\chi) + 4F'(\chi))}{3(F(\chi) - \chi F'(\chi))^2 F''(\chi)}
\end{aligned} \tag{70}$$

¹⁴In this paper, we adopt \simeq to represent slow-roll approximation.

$$\begin{aligned}
\frac{dn_s}{d \ln k} &\simeq 16\epsilon_V \eta_V - 24\epsilon_V^2 - 2\xi_V \\
&= \frac{-8[2F(\chi) - \chi F'(\chi)]}{9(F(\chi) - \chi F'(\chi))^4 F''(\chi)^3} \left[\chi^2 F'(\chi)^4 (F''(\chi)^2 - F^{(3)}(\chi) F'(\chi)) \right. \\
&\quad + 2\chi F(\chi) F'(\chi)^3 (F^{(3)}(\chi) F'(\chi) - 3F''(\chi)^2) \\
&\quad \left. + F(\chi)^2 F'(\chi) (3\chi F''(\chi)^3 - F^{(3)}(\chi) F'(\chi)^2 + 5F'(\chi) F''(\chi)^2) \right], \tag{71}
\end{aligned}$$

$$\begin{aligned}
\frac{dn_s^2}{d \ln k^2} &\simeq -192\epsilon_V^3 + 192\epsilon_V^2 \eta_V - 32\epsilon_V \eta_V^2 - 24\epsilon_V \xi_V + 2\eta_V \xi_V + 2\omega_V \\
&= \frac{16(\chi F'(\chi) - 2F(\chi))}{27(F(\chi) - \chi F'(\chi))^6} \left\{ 12(2F(\chi) - \chi F'(\chi))^5 \right. \\
&\quad - \frac{8(F(\chi) - \chi F'(\chi))^2 (\chi F'(\chi) - 2F(\chi)) (-4F(\chi) F''(\chi) + F'(\chi)^2 + \chi F'(\chi) F''(\chi))^2}{F''(\chi)^2} \\
&\quad - \frac{24(F(\chi) - \chi F'(\chi)) (\chi F'(\chi) - 2F(\chi))^3 (-4F(\chi) F''(\chi) + F'(\chi)^2 + \chi F'(\chi) F''(\chi))}{F''(\chi)} \\
&\quad - \frac{(F(\chi) - \chi F'(\chi))^3}{F''(\chi)^4} [-4F(\chi) F''(\chi) + F'(\chi)^2 + \chi F'(\chi) F''(\chi)] \\
&\quad \times \left(-8F(\chi) F''(\chi)^3 + F^{(3)}(\chi) F'(\chi)^3 + 3F'(\chi)^2 F''(\chi)^2 + \chi F'(\chi) F''(\chi)^3 \right) \\
&\quad - \frac{6(F(\chi) - \chi F'(\chi))^2 (\chi F'(\chi) - 2F(\chi))^2}{F''(\chi)^3} \left[-8F(\chi) F''(\chi)^3 + F^{(3)}(\chi) F'(\chi)^3 \right. \\
&\quad \left. + 3F'(\chi)^2 F''(\chi)^2 + \chi F'(\chi) F''(\chi)^3 \right] \\
&\quad + \frac{(F(\chi) - \chi F'(\chi))^3 (2F(\chi) - \chi F'(\chi))}{F''(\chi)^6} [-18F(\chi) F''(\chi)^6 \\
&\quad + 2F'(\chi) (\chi F''(\chi)^6 + 3F(\chi) F^{(3)}(\chi) F''(\chi)^4) \\
&\quad + F^{(3)}(\chi) F'(\chi)^3 (2F(\chi) F^{(3)}(\chi)^2 + 2F''(\chi)^3 + 3\chi F^{(3)}(\chi) F''(\chi)^2) \\
&\quad + F'(\chi)^2 (7F''(\chi)^5 - 3\chi F^{(3)}(\chi) F''(\chi)^4 - 6F(\chi) F^{(3)}(\chi)^2 F''(\chi)^2) \\
&\quad \left. \left. - F'(\chi)^4 (\chi F^{(3)}(\chi)^3 + F^{(4)}(\chi) F''(\chi)^2 - 3F^{(3)}(\chi)^2 F''(\chi)) \right] \right\}. \tag{72}
\end{aligned}$$

Also, the tensor spectral index and its running are given by

$$\begin{aligned}
n_t &\simeq -2\epsilon_V = \frac{-2[\chi F'(\chi) - 2F(\chi)]^2}{3[F(\chi) - \chi F'(\chi)]^2}, \\
\frac{dn_t}{d \ln k} &\simeq 4\epsilon_V \eta_V - 8\epsilon_V^2 \\
&= \frac{-8(\chi F'(\chi) - 2F(\chi))^2 [F(\chi) F'(\chi) (\chi F''(\chi) + F'(\chi)) - \chi F'(\chi)^3]}{9(F(\chi) - \chi F'(\chi))^4 F''(\chi)}, \tag{73}
\end{aligned}$$

and the tensor-to-scalar ratio is given by

$$r = \frac{P_s(k)}{P_t(k)} \simeq 16\epsilon_V = \frac{16 [\chi F'(\chi) - 2F(\chi)]^2}{3 [F(\chi) - \chi F'(\chi)]^2}. \quad (74)$$

where the scalar and tensor power spectra at a pivot scale k , $P_s(k)$ and $P_t(k)$ are given by

$$P_s(k) = \frac{1}{24\pi^2 M_{\text{pl}}^4} \frac{V}{\epsilon_V}, \quad P_t(k) = \frac{8}{M_{\text{pl}}^2} \left(\frac{H}{2\pi} \right)^2. \quad (75)$$

B Specific derivatives of BI-extended model

B.1 The BI-extended model and its derivatives

Given that our model is

$$F(R) = R + \frac{2g^2}{3\beta} \left(\sqrt{1 + 12\beta R^2} - 1 \right), \quad (76)$$

the first, second, third, fourth and fifth derivatives of $F(R)$ are

$$F'(R) := F^{(1)}(R) = 1 + \frac{8g^2 R}{\sqrt{1 + 12\beta R^2}}, \quad (77)$$

$$F''(R) := F^{(2)}(R) = \frac{8g^2}{(12\beta R^2 + 1)^{\frac{3}{2}}}, \quad (78)$$

$$F'''(R) := F^{(3)}(R) = -\frac{288\beta g^2 R}{(12\beta R^2 + 1)^{5/2}}, \quad (79)$$

$$F''''(R) := F^{(4)}(R) = \frac{288\beta g^2 (48\beta R^2 - 1)}{(12\beta R^2 + 1)^{7/2}}, \quad (80)$$

$$F'''''(R) := F^{(5)}(R) = -\frac{51840\beta^2 g^2 R (16\beta R^2 - 1)}{(12\beta R^2 + 1)^{9/2}}. \quad (81)$$

B.2 $\frac{d\chi}{d\phi}$ and its derivatives

$\frac{d\chi}{d\phi}$ and its derivatives are given by

$$\frac{d\chi}{d\phi} = \left(\frac{1}{M_{\text{pl}}} \sqrt{\frac{2}{3}} \right) \frac{(12\beta\chi^2 + 1)}{8g^2} \left(8g^2\chi + \sqrt{12\beta\chi^2 + 1} \right), \quad (82)$$

$$\frac{d}{d\chi} \left(\frac{d\chi}{d\phi} \right) = \left(\frac{1}{M_{\text{pl}}} \sqrt{\frac{2}{3}} \right) \left[\frac{9\beta\chi}{2g^2} \sqrt{12\beta\chi^2 + 1} + 36\beta\chi^2 + 1 \right], \quad (83)$$

$$\frac{d^2}{d\chi^2} \left(\frac{d\chi}{d\phi} \right) = \left(\frac{1}{M_{\text{pl}}} \sqrt{\frac{2}{3}} \right) \frac{9\beta \left(16g^2\chi\sqrt{12\beta\chi^2+1} + 24\beta\chi^2 + 1 \right)}{2g^2\sqrt{12\beta\chi^2+1}}, \quad (84)$$

$$\frac{d^3}{d\chi^3} \left(\frac{d\chi}{d\phi} \right) = \left(\frac{1}{M_{\text{pl}}} \sqrt{\frac{2}{3}} \right) 18\beta \left[\frac{9\beta\chi(8\beta\chi^2+1)}{g^2(12\beta\chi^2+1)^{3/2}} + 4 \right]. \quad (85)$$

B.3 Potential V and its derivatives with respect to χ

Based on the specific model, the potential is given by

$$V(\chi) = \frac{g^2 M_{\text{pl}}^2 \sqrt{12\beta\chi^2+1} \left(\sqrt{12\beta\chi^2+1} - 1 \right)}{3\beta \left(\sqrt{12\beta\chi^2+1} + 8g^2\chi \right)^2}, \quad (86)$$

$$V'(\chi) = \frac{4g^2 M_{\text{pl}}^2 \left[3\beta\chi\sqrt{12\beta\chi^2+1} - 4g^2 \left(-6\beta\chi^2 + \sqrt{12\beta\chi^2+1} - 1 \right) \right]}{3\beta\sqrt{12\beta\chi^2+1} \left(\sqrt{12\beta\chi^2+1} + 8g^2\chi \right)^3}, \quad (87)$$

$$\begin{aligned} V''(\chi) = & \frac{4g^2 M_{\text{pl}}^2}{\beta(12\beta\chi^2+1)^{3/2} \left(\sqrt{12\beta\chi^2+1} + 8g^2\chi \right)^4} \left[-288\beta^3\chi^4 - 12\beta^2\chi^2 + \beta \right. \\ & + 32g^4 \left(-48\beta^2\chi^4 + 6\beta\chi^2 \left(2\sqrt{12\beta\chi^2+1} - 3 \right) + \sqrt{12\beta\chi^2+1} - 1 \right) \\ & \left. - 16\beta g^2\chi \left(12\beta\chi^2 \left(2\sqrt{12\beta\chi^2+1} - 3 \right) + 4\sqrt{12\beta\chi^2+1} - 3 \right) \right], \end{aligned} \quad (88)$$

and $V'''(\chi)$, $V''''(\chi)$ can also be evaluated similarly.

B.4 Derivatives of the potential V with respect to ϕ

The derivatives of the potential V with respect to ϕ in terms of χ are given by

$$\frac{dV}{d\phi} = \frac{M_{\text{pl}}\sqrt{72\beta\chi^2+6}}{18\beta \left(\sqrt{12\beta\chi^2+1} + 8g^2\chi \right)^2} \left\{ 3\beta\chi\sqrt{12\beta\chi^2+1} - 4g^2 \left(-6\beta\chi^2 + \sqrt{12\beta\chi^2+1} - 1 \right) \right\}, \quad (89)$$

$$\begin{aligned} \frac{d^2V}{d\phi^2} = & \frac{1}{72\beta g^2 \left(\sqrt{12\beta\chi^2+1} + 8g^2\chi \right)^2} \left\{ 3\beta(12\beta\chi^2+1)^{5/2} \right. \\ & + 64g^4\sqrt{12\beta\chi^2+1} \left(36\beta^2\chi^4 - 6\beta\chi^2 + \sqrt{12\beta\chi^2+1} - 1 \right) \\ & \left. + 24\beta g^2\chi(12\beta\chi^2+1)(24\beta\chi^2-1) \right\}, \end{aligned} \quad (90)$$

and $\frac{d^3V}{d\phi^3}$, $\frac{d^4V}{d\phi^4}$ can also be evaluated similarly.

C Specific derivatives of Starobinsky model

C.1 Derivatives

Given that the Starobinsky model is given by

$$F(R) = R + 4g^2 R^2, \quad (91)$$

the first and second derivatives of $F(R)$ are

$$F'(R) := F^{(1)}(R) = 1 + 8g^2 R, \quad (92)$$

$$F''(R) := F^{(2)}(R) = 8g^2, \quad (93)$$

while the derivatives of $F(R)$ higher than the second order with respect to R vanish. The relationship between R and the inflaton field ϕ is given by

$$F'(R) = e^{\sqrt{\frac{2}{3}} \frac{\phi}{M_{\text{pl}}}} \Rightarrow R = \frac{1}{8g^2} \left(e^{\sqrt{\frac{2}{3}} \frac{\phi}{M_{\text{pl}}}} - 1 \right). \quad (94)$$

C.2 $\frac{d\chi}{d\phi}$ and its derivatives

$\frac{d\chi}{d\phi}$ and its derivatives are given by

$$\frac{d\chi}{d\phi} = \left(\frac{1}{M_{\text{pl}}} \sqrt{\frac{2}{3}} \right) \frac{1 + 8g^2 \chi}{8g^2}, \quad \frac{d}{d\chi} \left(\frac{d\chi}{d\phi} \right) = \left(\frac{1}{M_{\text{pl}}} \sqrt{\frac{2}{3}} \right), \quad (95)$$

while the derivatives of $\frac{d\chi}{d\phi}$ higher than the first order with respect to χ vanish.

C.3 Potential V and its derivatives with respect to χ

Based on the Starobinsky model, the potential and its derivatives are given by

$$V(\chi) = \frac{2g^2 \chi^2 M_{\text{pl}}^2}{(8g^2 \chi + 1)^2}, \quad (96)$$

$$V'(\chi) = \frac{4g^2 \chi M_{\text{pl}}^2}{(8g^2 \chi + 1)^3}, \quad (97)$$

$$V''(\chi) = - \frac{4g^2 (16g^2 \chi - 1) M_{\text{pl}}^2}{(8g^2 \chi + 1)^4}, \quad (98)$$

$$V'''(\chi) = \frac{192g^4 (8g^2 \chi - 1) M_{\text{pl}}^2}{(8g^2 \chi + 1)^5}, \quad (99)$$

$$V''''(\chi) = - \frac{3072g^6 (16g^2 \chi - 3) M_{\text{pl}}^2}{(8g^2 \chi + 1)^6}. \quad (100)$$

C.4 Derivatives of the potential V with respect to ϕ

The derivatives of the potential V with respect to ϕ in terms of χ are given by

$$\frac{dV}{d\phi} = \frac{dV}{d\chi} \frac{d\chi}{d\phi} = \frac{M_{\text{pl}}\chi}{\sqrt{6}(8g^2\chi + 1)^2}, \quad (101)$$

$$\frac{d^2V}{d\phi^2} = \frac{1 - 8g^2\chi}{24g^2(8g^2\chi + 1)^2}, \quad (102)$$

$$\frac{d^3V}{d\phi^3} = \frac{8g^2\chi - 3}{12\sqrt{6}g^2(8g^2\chi + 1)^2 M_{\text{pl}}}, \quad (103)$$

$$\frac{d^4V}{d\phi^4} = \frac{7 - 8g^2\chi}{36g^2(8g^2\chi + 1)^2 M_{\text{pl}}^2}. \quad (104)$$

C.5 Slow roll parameters in terms of χ

The slow roll parameters in terms of χ are given by

$$\epsilon_V(\chi) = \frac{1}{48g^4\chi^2}, \quad \eta_V(\chi) = \frac{1 - 8g^2\chi}{48g^4\chi^2}, \quad \xi_V(\chi) = \frac{8g^2\chi - 3}{288g^6\chi^3}, \quad \omega_V(\chi) = \frac{7 - 8g^2\chi}{1728g^8\chi^4}. \quad (105)$$

The scalar spectral index and its runnings in terms of χ are given by

$$n_s \simeq 1 + 2\eta_V - 6\epsilon_V = -\frac{1}{12g^4\chi^2} - \frac{1}{3g^2\chi} + 1, \quad (106)$$

$$\frac{dn_s}{d\ln k} \simeq 16\epsilon_V\eta_V - 24\epsilon_V^2 - 2\xi_V = -\frac{16g^4\chi^2 + 10g^2\chi + 1}{288g^8\chi^4}, \quad (107)$$

$$\begin{aligned} \frac{d^2n_s}{d\ln k^2} &\simeq -192\epsilon_V^3 + 192\epsilon_V^2\eta_V - 32\epsilon_V\eta_V^2 - 24\epsilon_V\xi_V + 2\eta_V\xi_V + 2\omega_V \\ &= -\frac{128g^6\chi^3 + 136g^4\chi^2 + 31g^2\chi + 2}{6912g^{12}\chi^6}. \end{aligned} \quad (108)$$

The scalar power spectrum evaluated at the first horizon crossing is given by

$$A_s = P_s(k_{\text{hc}}) \simeq \frac{1}{24\pi^2 M_{\text{pl}}^4} \frac{V(\chi_{\text{hc}})}{\epsilon_V(\chi_{\text{hc}})} = \frac{4g^6\chi^4}{\pi^2 M_{\text{pl}}^2 (8g^2\chi + 1)^2} \Big|_{\chi=\chi_{\text{hc}}}. \quad (109)$$

Also, the tensor spectral index and its runnings in terms of χ are given by

$$n_t \simeq -2\epsilon_V = -\frac{1}{24g^4\chi^2}, \quad (110)$$

$$\frac{dn_t}{d\ln k} \simeq 4\epsilon_V\eta_V - 8\epsilon_V^2 = -\frac{8g^2\chi + 1}{576g^8\chi^4}, \quad (111)$$

and the tensor-to-scalar ratio in terms of χ is given by

$$r \simeq 16\epsilon_V = \frac{1}{3g^4\chi^2}. \quad (112)$$

C.6 Slow roll parameters in terms of ϕ

The slow roll parameters in terms of ϕ are given by

$$\begin{aligned}\epsilon_V(\phi) &= \frac{4}{3} \left(e^{\sqrt{\frac{2}{3}} \frac{\phi}{M_{\text{pl}}}} - 1 \right)^{-2}, & \eta_V(\phi) &= \frac{-4 \left(e^{\sqrt{\frac{2}{3}} \frac{\phi}{M_{\text{pl}}}} - 2 \right)}{3 \left(e^{\sqrt{\frac{2}{3}} \frac{\phi}{M_{\text{pl}}}} - 1 \right)^2}, \\ \xi_V(\phi) &= \frac{16 \left(e^{\sqrt{\frac{2}{3}} \frac{\phi}{M_{\text{pl}}}} - 4 \right)}{9 \left(e^{\sqrt{\frac{2}{3}} \frac{\phi}{M_{\text{pl}}}} - 1 \right)^3}, & \omega_V(\phi) &= \frac{-64 \left(e^{\sqrt{\frac{2}{3}} \frac{\phi}{M_{\text{pl}}}} - 8 \right)}{27 \left(e^{\sqrt{\frac{2}{3}} \frac{\phi}{M_{\text{pl}}}} - 1 \right)^4}.\end{aligned}\tag{113}$$

The scalar spectral index and its runnings in terms of ϕ are given by

$$n_s \simeq 1 + 2\eta_V - 6\epsilon_V = \frac{-14e^{\sqrt{\frac{2}{3}} \frac{\phi}{M_{\text{pl}}}} + 3e^{2\sqrt{\frac{2}{3}} \frac{\phi}{M_{\text{pl}}}} - 5}{3 \left(e^{\sqrt{\frac{2}{3}} \frac{\phi}{M_{\text{pl}}}} - 1 \right)^2},\tag{114}$$

$$\frac{dn_s}{d \ln k} \simeq 16\epsilon_V \eta_V - 24\epsilon_V^2 - 2\xi_V = \frac{-32e^{\sqrt{\frac{2}{3}} \frac{\phi}{M_{\text{pl}}}} \left(e^{\sqrt{\frac{2}{3}} \frac{\phi}{M_{\text{pl}}}} + 3 \right)}{9 \left(e^{\sqrt{\frac{2}{3}} \frac{\phi}{M_{\text{pl}}}} - 1 \right)^4},\tag{115}$$

$$\begin{aligned}\frac{d^2 n_s}{d \ln k^2} &\simeq -192\epsilon_V^3 + 192\epsilon_V^2 \eta_V - 32\epsilon_V \eta_V^2 - 24\epsilon_V \xi_V + 2\eta_V \xi_V + 2\omega_V \\ &\quad - 128e^{\sqrt{\frac{2}{3}} \frac{\phi}{M_{\text{pl}}}} \left(11e^{\sqrt{\frac{2}{3}} \frac{\phi}{M_{\text{pl}}}} + 2e^{2\sqrt{\frac{2}{3}} \frac{\phi}{M_{\text{pl}}}} + 3 \right) \\ &= \frac{\hspace{10em}}{27 \left(e^{\sqrt{\frac{2}{3}} \frac{\phi}{M_{\text{pl}}}} - 1 \right)^6}.\end{aligned}\tag{116}$$

The scalar power spectrum evaluated at the first horizon crossing is given by

$$A_s = P_s(k_{\text{hc}}) \simeq \frac{1}{24\pi^2 M_{\text{pl}}^4} \frac{V(\phi_{\text{hc}})}{\epsilon_V(\phi_{\text{hc}})} = \frac{1}{1024\pi^2 g^2 M_{\text{pl}}^2} e^{2\sqrt{\frac{2}{3}} \frac{\phi}{M_{\text{pl}}}} \left(1 - e^{-\sqrt{\frac{2}{3}} \frac{\phi}{M_{\text{pl}}}} \right)^4 \Big|_{\phi=\phi_{\text{hc}}}.\tag{117}$$

Also, the tensor spectral index and its runnings in terms of ϕ are given by

$$n_t \simeq -2\epsilon_V = \frac{-8}{3} \left(e^{\sqrt{\frac{2}{3}} \frac{\phi}{M_{\text{pl}}}} - 1 \right)^{-2},\tag{118}$$

$$\frac{dn_t}{d \ln k} \simeq 4\epsilon_V \eta_V - 8\epsilon_V^2 = \frac{-64}{9} e^{\sqrt{\frac{2}{3}} \frac{\phi}{M_{\text{Pl}}}} \left(e^{\sqrt{\frac{2}{3}} \frac{\phi}{M_{\text{Pl}}}} - 1 \right)^{-4}, \quad (119)$$

and the tensor-to-scalar ratio in terms of ϕ is given by

$$r(\phi) \simeq \frac{64}{3} \left(e^{\sqrt{\frac{2}{3}} \frac{\phi}{M_{\text{Pl}}}} - 1 \right)^{-2}. \quad (120)$$

D Data points for the $n_{RR} - r$ graph

In this part, all the data points (n_s, r) (TT,TE,EE+lowE+lensing) with marginalized joint 68% CL in the $n_s - r$ graph Fig.(7) are listed in Table 3.

Nothing (Gray)	BK14 (Red)	BK14+BAO (Blue)
(0.958208, 0)	(0.959498, 0)	(0.962079, 0)
(0.958638, 0.00819672)	(0.95914, 0.00819672)	(0.961649, 0.00819672)
(0.95914, 0.0163934)	(0.959283, 0.0163934)	(0.961505, 0.0163934)
(0.959857, 0.026776)	(0.959857, 0.026776)	(0.961935, 0.026776)
(0.960645, 0.036612)	(0.960789, 0.036612)	(0.962724, 0.036612)
(0.961219, 0.0445355)	(0.962007, 0.0445355)	(0.963799, 0.0445355)
(0.961935, 0.05)	(0.963656, 0.05)	(0.965233, 0.05)
(0.962939, 0.0565574)	(0.966237, 0.0543716)	(0.967742, 0.0543716)
(0.964301, 0.0642077)	NaN	NaN
(0.966667, 0.0688525)	NaN	NaN
(0.96853, 0.0642077)	NaN	NaN
(0.969534, 0.0565574)	NaN	NaN
(0.970179, 0.05)	(0.968244, 0.05)	(0.969821, 0.05)
(0.970538, 0.0445355)	(0.969391, 0.0445355)	(0.970824, 0.0445355)
(0.971039, 0.036612)	(0.970251, 0.036612)	(0.971541, 0.036612)
(0.97147, 0.026776)	(0.970824, 0.026776)	(0.972043, 0.026776)
(0.971756, 0.0163934)	(0.970824, 0.0163934)	(0.972115, 0.0163934)
(0.971971, 0.00819672)	(0.970394, 0.00819672)	(0.971685, 0.00819672)
(0.972258, 0)	(0.969821, 0)	(0.970824, 0)

Table 3: Data points (TT,TE,EE+lowE+lensing) with marginalized joint 68% CL in the $n_{RR} - r$ graph of Planck 2018

References

- [1] D. Baumann, L. McAllister, *Inflation and String Theory*, Cambridge Monograph on Mathematical Physics, Cambridge University Press, 2015, doi:10.1017/CBO9781316105733

- [2] Dmitry S. Gorbunov, Valery A Rubakov, *Introduction to the Theory of the Early Universe: Cosmological Perturbations and Inflationary Theory*, World Scientific Publishing Co Pte Ltd, 2011, doi:10.1142/7873
- [3] Alan H. Guth, *Inflationary universe: A possible solution to the horizon and flatness problems*, Phys. Rev. D23 (1981), 347-356
- [4] A. A. Starobinsky, *A new type of isotropic cosmological models without singularity*, Phys. Lett. B91 (1980), 99-102
- [5] K. Sato, *First-order phase transition of a vacuum and the expansion of the Universe*, Mon. Not. Roy. Astron. Soc. 195 (1981), 467-479
- [6] Planck Collaboration: P.A.R. Ade, et al, *Planck 2013 results. XXII. Constraints on inflation*, Astron. Astrophys. 571 (2014) A22, arXiv: 1303.5082
- [7] Planck Collaboration: Y. Akrami, et al, *Planck 2018 results. X. Constraints on inflation*, 2018, arXiv: 1807.06211
- [8] Jerome Martin, Christophe Ringeval, Vincent Vennin, *Encyclopaedia Inflationaris*, Phys.Dark Univ. 5-6 (2014), 75-235, arXiv: 1303.3787
- [9] Mukhanov, V. F., Chibisov, G., *Quantum Fluctuation and Nonsingular Universe (In Russian)*, 1981, JETP Lett., 33, 532
- [10] Starobinsky, A., *The Perturbation Spectrum Evolving from a Nonsingular Initially de Sitter Cosmology and the Microwave Background Anisotropy*, 1983, Sov. Astron. Lett., 9, 302
- [11] S. Nojiri, S.D. Odintsov, V.K. Oikonomou, *Modified Gravity Theories on a Nutshell: Inflation, Bounce and Late-time Evolution*, Phys.Rept. 692 (2017) 1-104, arXiv: 1705.11098
- [12] L. Sebastiani, G. Cognola, R.Myrzakulov, S.D. Odintsov, S. Zerbini, *Nearly Starobinsky inflation from modified gravity*, Phys. Rev. D 89, 023518 (2014), arXiv: 1311.0744
- [13] L. Sebastiani, G. Cognola, R.Myrzakulov, S.D. Odintsov, S. Zerbini, *Spotting deviations from R^2 inflation*, JCAP 05 (2016) 060, arXiv:1603.05537
- [14] S.D. Odintsov, V.K. Oikonomou, *Singular deformations of nearly R^2 inflation potentials*, arXiv: 1504.01772
- [15] S.D. Odintsov, V.K. Oikonomou, L. Sebastiani, *Unification of Constant-roll Inflation and Dark Energy with Logarithmic R^2 -corrected and Exponential $F(R)$ Gravity*, Nucl. Phys. B Vol. 923 (2017) 608-632, arXiv: 1708.08346
- [16] Renata Kallosh, Andrei Linde, Diederik Roest, *Superconformal Inflationary α - Attractors*, JHEP 11 (2013) 198, arXiv: 1311.0472

- [17] Renata Kallosh, Andrei Linde, Diederik Roest, Timm Wrase, *Sneutrino Inflation with α - Attractors*, JCAP 1611 (2016) 046, arXiv: 1607.08854
- [18] S.D. Odintsov, V.K. Oikonomou, *Inverse Symmetric Inflationary Attractors*, Classical and Quantum Gravity Vol. 34, No.10, 2017, arXiv: 1611.00738
- [19] S.D. Odintsov, V.K. Oikonomou, *Inflationary α - attractors from $F(R)$ Gravity*, Phys. Rev. D 94 (2016) 124026, arXiv: 1612.01126
- [20] Renata Kallosh, Andrei Linde, Diederik Roest, Alexander Westphal, Yusuke Yamada, *Fibre Inflation and α - attractors*, JHEP 02 (2018) 117, arXiv: 1707.05830
- [21] Yashar Akrami, Renata Kallosh, Andrei Linde, Valeri Vardanyan, *Dark energy, α - attractors, and Large-scale structure surveys*, JCAP 1806 (2018) 041, arXiv: 1712.09693
- [22] Edmund J. Copeland, Andrew R. Liddle, David H. Lyth, Ewan D. Stewart, David Wands, *False vacuum inflation with Einstein gravity*, Phys. Rev. D 49 (1994), 6410-6433, arXiv: astro-ph/9401011
- [23] M. Kawasaki, Masahide Yamaguchi, T. Yanagida, *Natural chaotic inflation in supergravity*, Phys. Rev. Lett. 85 (2000), 3572-3575, arXiv: hep-ph/0004243
- [24] Renata Kallosh, Andrei Linde, Tomas Rube, *General inflaton potentials in supergravity*, Phys. Rev. D 83 (2011), 043507, arXiv: 1011.5945
- [25] Sergio Ferrara, Renata Kallosh, Andrei Linde, Massimo Porrati, *Minimal supergravity models of inflation*, Phys. Rev. D 88 (2013), 085038, arXiv: 1307.7696
- [26] Fotis Farakos, Rikard von Unge, *Naturalness and chaotic inflation in supergravity models of inflation*, JHEP 08(2014)168, arXiv: 1404.3739
- [27] Max Born and L. Infeld, *Foundations of the new field theory*, Proc. R. Soc. A 144, 425 (1934)
- [28] P.A.M. Dirac, *An extensible model of the electron*, Proc. R. Soc. A 268, 57 (1962)
- [29] S. Cecotti, S. Ferrara, *Supersymmetric Born-infeld Lagrangians*, Phys. Lett. B Vol 187 Issue 3-4, 1987, 335-339
- [30] Jonathan Bagger, Alexander Galperin, *New Goldstone multiplet for partially broken supersymmetry*, Phys.Rev.D55 (1997), 1091-1098, arXiv: hep-th/9608177
- [31] Shin'ichi Nojiri, Sergei D. Odintsov, *Unified cosmic history in modified gravity: from $F(R)$ theory to Lorentz non-invariant models*, Phys.Rept. 505 (2011) 59-144, arXiv: 1011.0544
- [32] F. Farakos, A. Kehagias, A. Riotto, *On the Starobinsky model of inflation from supergravity*, Nucl. Phys. B876, 187 (2013), arXiv: 1307.1137

- [33] Hiroyuki Abe, Yutaka Sakamura, Yusuke Yamada, *Matter coupled Dirac-Born-Infeld action in 4 dimensional $\mathcal{N} = 1$ conformal supergravity*, Phys. Rev. D 92, 025017 (2015), arXiv: 1504.01221
- [34] Hiroyuki Abe, Yutaka Sakamura, Yusuke Yamada, *Massive vector multiplet inflation with Dirac-Born-Infeld type action*, Phys. Rev. D 91, 125042 (2015), arXiv: 1505.02235
- [35] Yermek Aldabergenov, Ryotaro Ishikawa, Sergei V. Ketov, Sergey I. Kruglov, *Beyond Starobinsky Inflation*, Phys. Rev. D 98, 083511 (2018), arXiv: 1807.08394
- [36] Swagat S. Mishra, Varun Sahni, Alexey V. Toporensky, *Initial conditions for Inflation in an FRW Universe*, Phys. Rev. D 98, 083538 (2018), arXiv: 1801.04948
- [37] Sergio Ferrara, Renata Kallosh, Antoine Van Proeyen, Timm Wrase, *Linear versus non-linear supersymmetry, in general*, JHEP04 065 (2018), arXiv: 1603.02653
- [38] Gia Dvali and S.-H. Henry Tye, *Brane inflation*, Phys. Lett. B450 (1999) 72-82, arXiv: hep-ph/9812483
- [39] Eva Silverstein, David Tong, *Scalar speed limits and cosmology: Acceleration from D-acceleration*, Phys. Rev. D 70 (2004), 103505, arXiv: hep-th/0310221